MRC—SL—341

FINAL REPORT

MAGNETIC BUBBLE MATERIALS

Monsanto Research Corporation
St. Louis, Missouri 63166
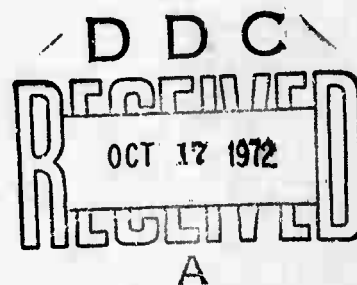
Jerry W. Moody, Robert M. Sandfort, and Roger W. Shaw

Contract No. DAAH01-72-C-0490

Distribution of this document is unlimited

ARPA Support Office
Research, Development, Engineering,
and Missile Systems Laboratory
U.S. Army Missile Command
Redstone Arsenal, Alabama

DDC

RECEIVED
OCT 17 1972

A

DOCUMENT CONTROL DATA - R & D

(Security classification of title, body of abstract and indexing annotation must be entered when the overall report is classified)

1 ORIGINATING ACTIVITY *(Corporate author)*	2a. REPORT SECURITY CLASSIFICATION
Monsanto Research Corporation 800 North Lindbergh Boulevard St. Louis, Missouri 63166	UNCLASSIFIED
	2b. GROUP

3 REPORT TITLE

MAGNETIC BUBBLE MATERIALS

4 DESCRIPTIVE NOTES *(Type of report and inclusive dates)*

FINAL REPORT (January 11, 1972 through July 11, 1972)

5 AUTHOR(S) *(First name, middle initial, last name)*

JERRY W. MOODY
ROBERT M. SANDFORT
ROGER W. SHAW

6 REPORT DATE	7a. TOTAL NO. OF PAGES	7b. NO. OF REFS
August 11, 1972	84	19

8a. CONTRACT OR GRANT NO	9a. ORIGINATOR'S REPORT NUMBER(S)
DAAH01-72-C-0490	MRC-SL-341
b. PROJECT NO. ARPA Order No. 1999-72	
c.	9b. OTHER REPORT NO(S) *(Any other numbers that may be assigned this report)*
d.	

10 DISTRIBUTION STATEMENT

Distribution of this document unlimited

11 SUPPLEMENTARY NOTES	12. SPONSORING MILITARY ACTIVITY
	Advanced Research Project Agency Washington, D.C.

13 ABSTRACT

The object of this project was to establish a reliable supply of high quality magnetic bubble materials to support the device work of various Department of Defense Agencies. This work included bulk, non-magnetic garnet crystal growth (for use as substrates), substrate polishing and preparation, and liquid phase epitaxial growth of a number of high performance, magnetic garnet compositions. Bulk, single crystals of $Gd_3Ga_5O_{12}$ were grown by the Czochralski method. Crystals containing low dislocation densities were routinely grown and some progress was made toward eliminating the strain "core" of such crystals by employing high crystal rotation rates. Procedures were established for polishing (111) wafers sliced from the $Gd_3Ga_5O_{12}$ crystals. Work damage-free surfaces, which proved excellent for epitaxial film growth, were produced by a process involving a final polish on a Syton-flooded, Corfam lap. Epitaxial films of six different compositions were deposited on (111) $Gd_3Ga_5O_{12}$ substrates from solution in $PbO-B_2O_3$ solvent by the simple "dipping" method. Solution recipes and growth conditions for each composition are discussed in detail in this report. Some general characteristics of the $PbO-B_2O_3$ solvent are described and the $PbO-B_2O_3$ solvent are described and the $PbO-B_2O_3$ and $BaO-F_2-B_2O_3$ solvent systems are compared.

1a

DD FORM 1473
1 NOV 65

14. KEY WORDS	LINK A		LINK B		LINK C	
	ROLE	WT	ROLE	WT	ROLE	WT
Magnetic bubble materials						
Magnetic garnets						
Gadolinium gallium garnets						
Crystal growth						
Liquid phase epitaxy						
Substrate preparation						
Super V garnets						
Rare earth iron garnets						
Super VIII garnets						

16

FINAL REPORT

MAGNETIC BUBBLE MATERIALS

Monsanto Research Corporation
St. Louis, Missouri 63166

Jerry W. Moody, Robert M. Sandfort, and Roger W. Shaw

August 11, 1972

ic

SUMMARY

This is the Final Report on the project "Magnetic Bubble Materials Phase I", Contract No. DAAH01-72-C-0490. It covers the period January 11, 1972 through July 11, 1972.

The object of this project was to establish a reliable supply of high quality magnetic bubble materials to suppprt the device work of various Department of Defense Agencies. This work included bulk, non-magnetic garnet crystal growth (for use as substrates), substrate polishing and preparation, and liquid phase epitaxial growth of a number of high performance, magnetic garnet compositions.

Bulk, single crystals of $Gd_3 Ga_5 O_{12}$ were grown by the Czochralski method. Crystals containing low dislocation densities were routinely grown and some progress was made toward eliminating the strain "core" of such crystals by employing high crystal rotation rates.

Procedures were established for polishing (111) wafers sliced from the $Gd_3 Ga_5 O_{12}$ crystals. Work damage-free surfaces, which proved excellent for epitaxial film growth, were produced by a process involving a final polish on a Syton-flooded, Corfam lap.

Epitaxial films of six different compositions were deposited on (111) $Gd_3 Ga_5 O_{12}$ substrates from solution in $PbO-B_2O_3$ solvent by the simple "dipping" method. Solution recipes and growth conditions for each composition are discussed in detail in this report. Some general characteristics of the $PbO-B_2O_3$ solvent are described and the $PbO-B_2O_3$ and $BaO-F_2-B_2O_3$ solvent systems are compared.

TABLE OF CONTENTS

TABLE OF CONTENTS (Cont.)

LIST OF TABLES

LIST OF FIGURES

1. INTRODUCTION

The primary objective of the first phase of ARPA contract No. DAAH01-72-C-0490 was to fulfill a need for a supply of reproducible, low defect, high quality magnetic bubble materials to support the device work of various DOD agencies who are investigating the application of these materials for end uses of importance to the national security. This primary objective centered not only on satisfying the need for materials having the necessary quality and reproducibility, but included establishing a reliable supply and dependable delivery of such materials of various compositions, as dictated by investigations carried out concurrently at Monsanto and within certain DOD agencies. The material specifications, established at the beginning of the programs, which served as guidelines and goals during the course of the work are given in Table I. These properties are considered desirable in materials which are to be used in magnetic bubble devices. As the following technical discussion will indicate, Monsanto, in the films shipped to ARPA, has largely met or exceeded these specifications, where the intrinsic characteristics of the materials permitted. The following sections of this report are intended to discuss the procedures used by Monsanto to grow the high quality material delivered during this program. The key areas of bulk crystal growth, substrate polishing and preparation and LPE growth will be discussed first, followed by individual discussions of the different rare earth magnetic garnet "compositional families" investigated under this contract. Particular attention will

1

be given to several interesting facets of the bulk crystal and LPE film growth procedures observed in our laboratories but not yet reported in the literature.

Quite apart from the crystal growth expertise demonstrated during the program, the already robust Monsanto materials characterization facility was improved and expanded during the contract period. Presently, some sixteen different parameters are measured in every sample delivered to ARPA. These data are supplied in the form of a characterization sheet along with a thickness contour map and a defect map for every sample. Two characterization reports were prepared during this contract, the first of which covered the methods used to characterize substrates and magnetic films at Monsanto Co. at the beginning of the contract period[Ref. 1], while the second was a study of the state of the art in the characterization of bubble materials[Ref. 2]. This latter report included establishment of all the parameters required to be characterized, presentation of the known techniques for each of the methods of characterization, and identification of the recommended recommended characterization method for each item. In light of the existence of these two previous exhaustive reports, little discussion will be devoted to material characterization in this report. The primary emphasis here will be on crystal growth processes, and phenomenological results obtained in various garnet compositional families.

TABLE I

Desired Magnetic Bubble Material Specifications

Property	Desired Value
Bubble Diameter (d)	$5 \mu m$
Magnetization ($4 \pi M_s$)	150 - 200 gauss
Thickness (h)	$5 \mu m$
Mobility (μ)	200 cm/sec/Oe
Coercivity (H_c)	0.1 Oe
Anisotropy Field (H_a)	$2(4 \pi M_s) - 10(4 \pi M_s)$
Defect Density	$< 20 \, cm^2$

2.1 Introduction

An ideal single crystal non-magnetic garnet substrate for a magnetic-bubble epitaxial film must satisfy several stringent criteria. It must have both an excellent room-temperature lattice match and an excellent thermal expansion match to the film. Tolerances depend somewhat upon the type of anisotropy (growth- or strain-induced) desired. Although these tolerances have not been determined precisely, in general they appear to be more stringent in the case of garnets than for most epitaxial work. If there is a significant lattice or thermal expansion mismatch, the epitaxial film tends to crack or to contain so many defects at the film-substrate interface that domain propagation is hendered. However, for bubble films to exhibit stress-induced anisotropy, there must be a certain minimum mismatch between film and substrate. In addition, the substrate must be nearly free of strain, dislocations, striations, inclusions, and similar structural defects that can affect the structure of the epitaxial layer and subsequently impede domain motion. It must be of a useful cross sectional area, preferably ≥ 1 cm^2, so that a practical information storage capacity can be achieved in the epitaxial film. If the substrate is a mixed garnet it should be, of course, of a uniform composition and lattice parameter. Finally the substrate must be of an appropriate crystalline orientation to allow the growth of thin films that support magnetic bubbles.

The garnets which best satisfy the above criteria for today's magnetic-bubble films are the family of rare-earth gallium garnets, the one most used to date being gadolinium gallium garnet. The rare-earth and yttrium aluminum garnets have lattice constants and thermal expansion coefficients too small to match well to today's useful magnetic-bubble films. Both the gallium and aluminum garnets melt congruently and can be grown from the melt but the high melting points of the garnets and the reactivity of their melts require the use of iridium as a crucible. Since the melts (and the solids) "wet" iridium it is practically impossible to remove the solid from the crucible intact. Therefore, the Czochralski method in which the crystal is "pulled" from the melt, is the preferred crystal growth technique.

One aim of this program was to develop a source of defect-free, non-magnetic garnets to be used as substrates. Since $Gd_3 Ga_5 O_{12}$ had proven to be the most useful substrate at the inception of this work, attention was directed toward this material. The details of this phase of the program are discussed in this section.

2.2   Experimental

2.2.1 Crystal Growth Furnace

Figure 1 is a sketch of a typical crystal growth furnace used in this work. The furnace consists of an inner stabilized ZrO_2 tube and an outer wall of fused silica. The inner tube is both lined and wrapped with Zircar*

---

* Zircar is a trade-name of the Union Carbide Corporation.

Figure 1. Cross Section of Crystal Growth Furnace

Labels (top to bottom, right side):
- Pull Rod
- Fused Silica Plate
- ZrO$_2$ Tubing
- Coupling
- Zircar* Felt
- Fused Silica Tube
- Al$_2$O$_3$ Seed Holder
- Seed
- Crystal
- R F Coil
- Iridium Crucible
- ZrO$_2$ Pedestal
- Base Plate

Gas Inlet
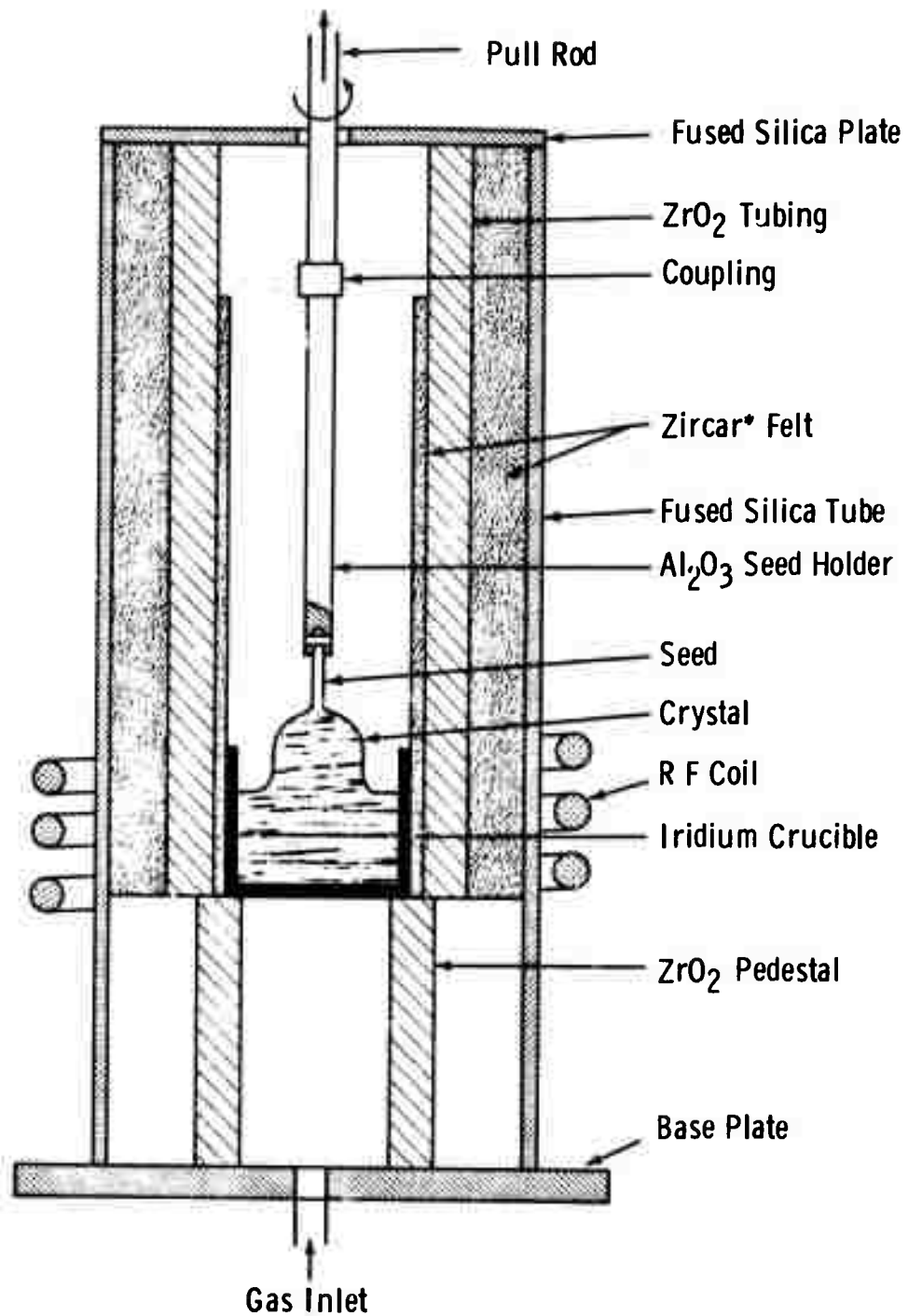
*Tradename of Union Carbide Corp.

left. The heat source is the iridium crucible which acts as a susceptor of the RF power coupled inductively from the water cooled coils wound around the outside furnace liner. The iridium crucible is supported upon a ZrO_2 pedistal. If growth in gases other than air is desired, these gases can be introduced through a port in the steel base plate and can flow out around the steel pull rod at the top of the furance. The seed is tied to the Al_2O_3 seed holder with Pt + 13% Rh wire.

The power source in use at the beginning of this project was a 10 kw Westinghouse RF generator which necessitated the use of a rather small furnace. The output of a Brown Radiamatic sensing head located on the base plate and focused on the bottom of the crucible was fed to a Leeds and North-rup proportional control system to control the generator. Later, a second furnace was constructed which used a 25 kw Westinghouse RF generator. The output of a pick-up coil fed to a Leeds and Northrup controller was used to control this generator. The two pulling chambers differed only in size and the amount of insulation which was packed between the inner and outer walls. The I.D. of the 10 kw furnace was 63mm and that of the 25 kw furnace was 75mm.

Iridium crucibles of two sizes were used in the 10 kw furnace: 1-1/4 inch I.D. x 1-1/4 inch high and 1-1/2 inch I.D. x 1-1/2 inch high. Only the larger crucible was used in the 25 kw furnace. Crucibles with and without reinforced lips were used in both furnaces. In general, better results were obtained in crucibles without the reinforced lip.

2.2.2 Starting Materials

Starting charges were prepared by mixing Gd_2O_3 and Ga_2O_3 powders in stoichiometric proportion. Gallium sesquioxide was obtained from Alusuisse Metals and from United Mineral and Chemical Corporation.

Gadolinium sesquioxide was obtained from United Mineral and Chemical Corporation and from Lindsay Rare Earths. The oxides were obtained in 99.99% purity.

After mixing, the powders were either pressed into cylindrical pellets (using a briqueting press) or poured directly into the crucible. In either case, several melt-downs were required to charge the crucible. In most cases the crucible was charged to about 3/4 of capacity.

2.2.3 Crystal Growth and Evaluation

All the $Gd_3 Ga_5 O_{12}$ crystals prepared on this program were grown on seeds oriented along the <111> direction. Pull rates of 4-8 mm/hr were used. The rotation rate was varied from 5 rpm to 50 rpm with most of the crystals being pulled at 10 or 20 rpm. The crystals were grown in an O_2 - N_2 atmosphere with the O_2 concentration varied from about 1 to 5 percent by volume. Total gas flow rates of 1200 - 1300 ml/min were used. The diameter of the crystal was usually kept to about one half the diameter of the crucible used in an effort to reduce thermal strains.

After growth, the ends of the crystals were cut off perpendicular to the growth axis. The ends were then polished flat and parallel so that the interior of the crystal could be examined. The crystals were examined visually for cracks, inclusions and voids, the extent and distribution of elastic strain was determined by examining the crystal between crossed polarizers.

If the boule appeared to be sound and free of inclusions, then the orientation of the crystal was determined by back-reflection X-ray procedures and (111) wafers were sliced from the front, middle and rear of the crystal. Certain of the wafers were used for precise lattice constant measurements. Others were etched for 5 minutes in ortho-phosphoric acid at 160 - 170°C. These wafers were then examined microscopically for dislocations, inclusions and growth striations. The wafers were then examined microscopically for dislocations, inclusions and growth striations. The wafers were examined in both transmitted and reflected light. The phase contrast microscope was particularly valuable in studying the "core" and growth striations in the etched wafers.

2.3 Results and Discussions

2.3.1 General

Figure 2 is a photograph of a group of typical $Gd_3 Ga_5 O_{12}$ crystals which were grown during this program. The ends of the crystals have been cropped in preparation for initial evaluation. The smaller crystals were grown in the 10 kw furnace using the smaller crucible and the two larger crystals were grown in the 25 kw furnace using the larger crucible.

The details concerning the crystals grown in the 10 kw furnace are summarized in Table II. All of these crystals were grown in an O_2 - N_2 atmosphere containing about 2 percent by volume O_2 and at a growth rate of about 7 mm/hr. In general, the defect density in these crystals was greater the faster the rotation rate used. However, none of these crystals

9
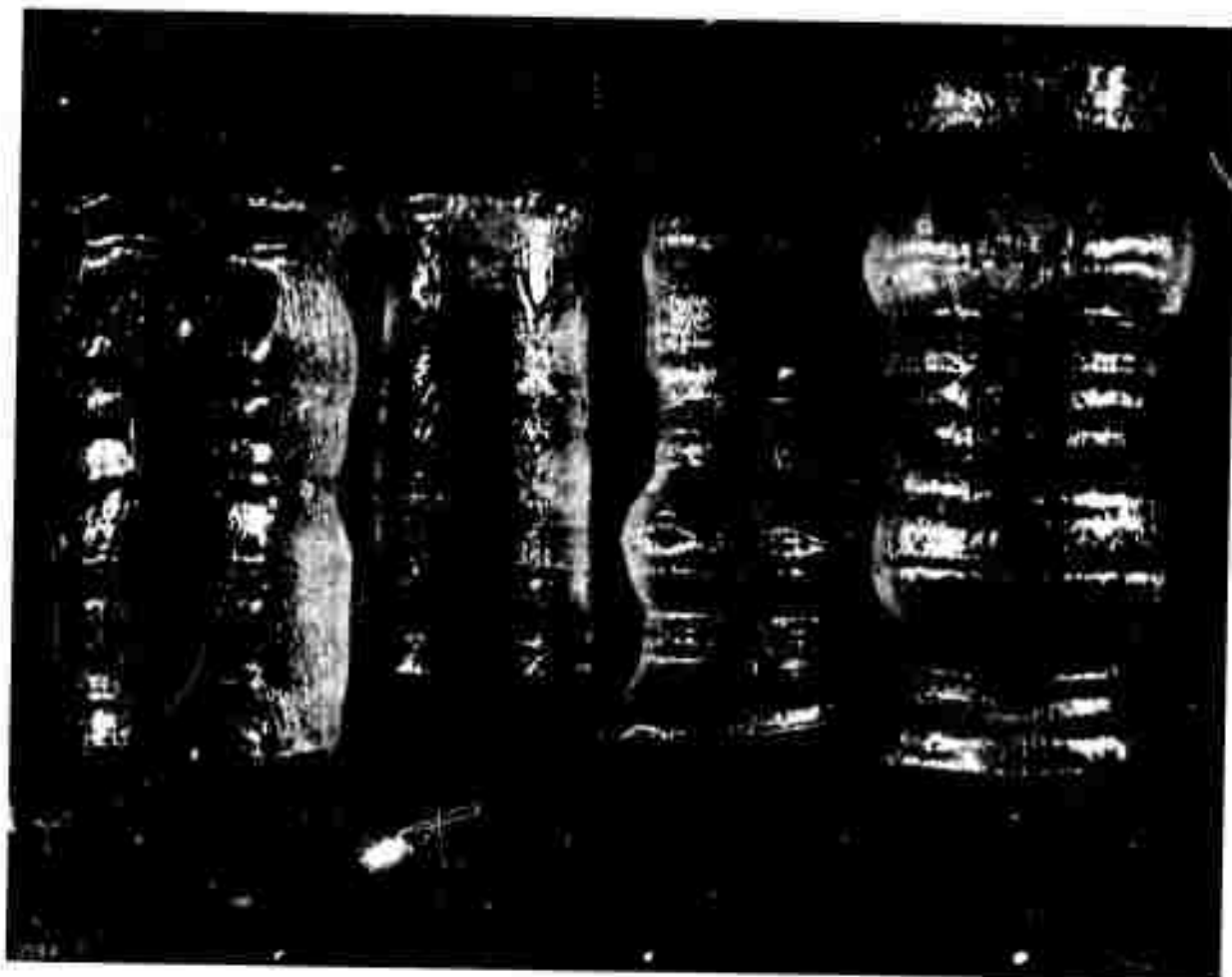
Figure 2.   Gadolinium Gallium Garnet Crystals

produced wafers with defect densities low enough to be used as substrates for device quality films. (On the other hand, the crystals did provide valuable substrates for exploratory work in adjusting solution/film compositions and determining film growth rates.) The defect densities found in these crystals could not be related unambigously to the growth conditions used. Therefore, it is believed that most of the defects were due to inadequate insulation in the relatively small 10 kw furnace. The growing crystal was exposed to large thermal gradients in the poorly insulated system and thermal stresses caused the high dislocation densities.

This conjecture is borne out by the results obtained in the 25 kw furnace. The details of these crystal growth runs are summarized in Table III. The 25 kw furnace accommodated about 1/4 inch more of the zirconia felt and, thus, was better insulated than the 10 kw furnace. The crystals grown in this system yielded, under certain growth conditions, wafers with essentially zero dislocation and inclusion densities. Such wafers were used as substrates for device quality films.

2.3.2 Strains

The relatively high thermal expansion coefficients of the rare earth garnets and the extreme temperature gradients in which the crystals are usually grown combine to produce highly strained crystals unless very special precautions are taken during the growth. One of the most characteristic and common defects found in Czochralski grown garnet crystals is a severely strained central "core". This central core

11

TABLE II

Summary of Crystal Growth Runs

10 kw Furnace

Crystal Number	Growth Rate (mm/hr)	Rotation Rate (rpm)	Lattice Constant (Å)	Remarks
4405	7	50	(F) 12.3818	Many dislocations scattered in groups
			(R) 12.3806	
4406	7	40	12.3833	Inclusions - bad striations
4407	7	15	(F) 12.3827	Center relatively defect free-many inclusions near outer edge
			(R) 12.3829	
4412	7	30	(F) 12.3832	Ir inclusions near front
			(R) 12.3837	
4414	7	20	-----	Used for seeds
4417	7	20	12.3871	Contaminated with Fe
4425	7	20	-----	Contaminated with Fe
4431	7	20	12.3840	Ir inclusions
4438	7	20	12.3822	Dislocations - Core
4441	7	20	12.3816	Dislocations - Core
4442	7	20	12.3830	Used for seeds
4445	5	20	12.3839	Many dislocations
4449	5	20	-----	Used for seeds
4452	5	10	12.3838	Core and striations
4455	5	10	-----	Used for seeds
4463	5	10	12.3837	Low dislocation density-many Ir inclusions
4488	5	5	-----	Bad core

(F) = front of crystal

(R) = rear of crystal

TABLE III

Summary of Crystal Growth Runs

25 kw Furnace

Crystal Number	Growth Rate (mm/hr)	Rotation Rate (rpm)	Lattice Constant (Å)	Remarks
4477	5	10	(F) 12.3341 (M) 12.3861 (R) 12.3865	Defect density $< 10 \text{cm}^{-2}$ strong core
4489	5	10	(F) 12.3836 (R) 12.3838	Defect density $< 10 \text{cm}^{-2}$ strong core
4490	5	10	(F) 12.3815 (R) 12.3842	Defect density $< 10 \text{cm}^{-2}$ strong core
4491	5	10	(F) 12.3817 (R) 12.3832	Defect density $< 10 \text{cm}^{-2}$ strong core
4492	5	30	12.3830	Defect density $> 10^3 \text{ cm}^{-2}$ weak core
4493	5	50	(F) 12.3829 (R) 12.3831	Defect density $> 10^4 \text{ cm}^{-2}$ weak core
4494	5	50	12.3809	Defect density $> 10^4 \text{ cm}^{-2}$ weak core
4500	5	10	-----	Used for seeds

(F) = front of crystal

(M) = middle of crystal

(R) = rear of crystal

13

is associated with the formation of (211) facets at the growth interface. In general, the interface between the growing crystal and the melt will not be planar, but either convex or concave to the melt. (For garnets the natural interface is concave to the melt.) Also, in general there is a steep longitudinal thermal gradient at the growth interface. This condition produces the strains in the crystal which result in the central core.

The non-planar interface results in another defect which is common in Czochralski grown garnet crystals. The defect is manifested as growth striations which can be observed by x-ray topography or by phase interference microscopy of etched surfaces. It is believed the striations correspond to periodic deviations in stoichiometry. In the central core region of garnets grown along the <111> direction the striations frequently assume a threefold symmetry. In the outer region of the crystal the striations more often appear as concentric circles centered about the growth axis. Strains and the central core can be observed by viewing the crystal between crossed polarizers. The striations can be observed by x-ray topography or by phase-interference microscopic examination of an etched surface.

Striations corresponding to those in the substrate will also be found in an epitaxially-grown magnetic film, especially one grown by liquid phase epitaxy (LPE). It is believed that the strained regions in the substrate are preferentially attacked and etched by the molten salt solvent used in LPE before film growth can occur. Under certain growth conditions (high temperatures, low supersaturation) the striations in the epitaxial film are

so pronounced that they impede the motion of magnetic domains. However, growth conditions can be adjusted so that the striations in the film are minimized and appear to have no pronounced effect on domain motion. Nevertheless, a strain-free, core-free wafer would be preferable and efforts were made to grow such material on this program.

Since the strains in the substrate are caused by a combination of a curved liquid/solid interface and steep thermal gradients, elimination of either should materially reduce or eliminate the striations. Thermal gradients at the interface can be reduced by use of after heaters and/or heat reflectors. However, if the thermal gradient is too low, constitutional supercooling can become a problem. On the other hand, the curved interface can be made planar by adjusting the rotation rate of the growing crystal. The core in $Y_3 Al_5 O_{12}$ was eliminated by Cockayne, et al[3] by increasing the normal rotation rate, about 10 rpm, to about 150 rpm. Similar results were recently obtained for $Gd_3 Ga_5 O_{12}$ by Brandle and Valentino[4] and by O'Kane and Sadagopan[5].

The rotation rate which will result in planar liquid/solid interface will depend upon relative diameters of the growing crystal and the crucible diameter, the growth rate, and the thermal gradients at the interface. In this work, rotation rates were varied from about 5 to 50 rpm (Tables II and III). The effect of rotation rate on the core and strain distribution in the crystals is illustrated in Figure 3 in which representative crystals are photographed between crossed polarizers. Crystal 4489 was grown at 10 rpm - the highly strained central core is obvious in Figure 3a. The core region is

15

a) Crystal 4489
Rotation Rate 10 RPM

b) Crystal 4492
Rotation Rate 30 RPM

c) Crystal 4494
Rotation Rate 50 RPM
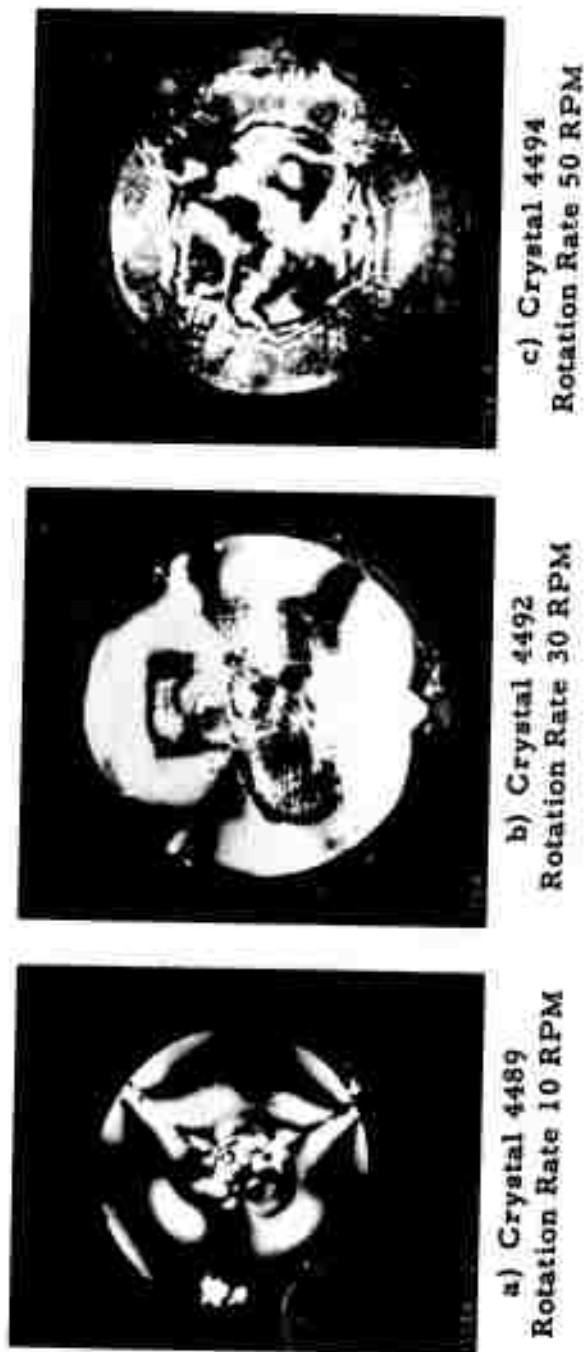
Figure 3.   Effect of Rotation Rate on Strain Distribution in $Gd_3 Ga_5 O_{12}$

expanded and is more diffuse in crystal 4492 which was grown at 30 rpm (Figure 3b). At 50 rpm the strain distribution becomes even more diffuse (Figure 3c). Phosphoric acid etching of wafers from crystals 4492 and 4494 did not reveal growth striations; however, the striations were apparent in etched wafers from crystal 4489.

It is evident from these results that the core region and growth striations can be eliminated by high rotation rates. However, the crystals grown at these rates contain high dislocation densities (Table III). The crystals grown at 10 rpm in the 25 kw furnace had dislocation densities of less than 10 cm^{-2} while the dislocation density of crystals grown at 30 or 50 rpm were 10^3 cm^{-2} or higher. This result was unexpected. It is now believed that slower growth rates must be used with the high rotation rate both to eliminate the core and to maintain a low dislocation density.

2.3.3 Inclusions

Gadolimium gallium garnet is not stable at its melting point (about 1700°C) in an inert atmosphere. The melts tend to loose gallium via a volatile suboxide[Ref. 6]. The decomposition of Ga_2O_3 can be suppressed by maintaining a partial pressure of oxygen above the melt. However, the melt is contained in an iridium crucible which is readily oxidized when in an oxygen atmosphere at elevated temperatures. It is difficult both to maintain melt stoichiometry and to minimize crucible oxidation simultaneously. During the long periods of time required to grow the crystals, the melt tends to become non-stoichiometric and saturated with IrO_2. It is not surprising,

therefore, that inclusions of one or more foreign phases are a common defect in garnet crystals.

Brandle, et al[Ref. 7] have discussed the origin and appearance of the most common inclusions found in $Gd_3 Ga_5 O_{12}$ crystals. Three types of inclusions were identified:

(1) triangular or hexagonal platelets of metallic iridium

(2) dark square or cubic crystals which are believed to be particles of gadolinium gallium suboxide, probably gadolinium orthogalliate $(GdGaO_3)$.

(3) transparent acicular crystals, tentatively identified as Gd_2O_3.

The first two types are by far the most predominant, with the third found only occasionally. Examples of the two most common defects are shown in the photomicrographs of Figure 4.

The occurrence of inclusions can be minimized by adjusting the composition of the ambient gas. The oxygen partial pressure should be high enough to suppress the decomposition of Ga_2O_3 but low enough to minimize oxidation of the crucible. In this work, satisfactory results were obtained with oxygen concentrations ranging from about 1.5 to 5.0 percent by volume. However, even with strict atmosphere control the melts tend to become non-stiochiometric during the long times which are required to grow a crystal. That portion of the melt next to the wall of the crucible is much hotter than the melt at the solid/liquid interface and $Ga_2 O_3$ can be decomposed on the hot walls. It is not uncommon for the

18
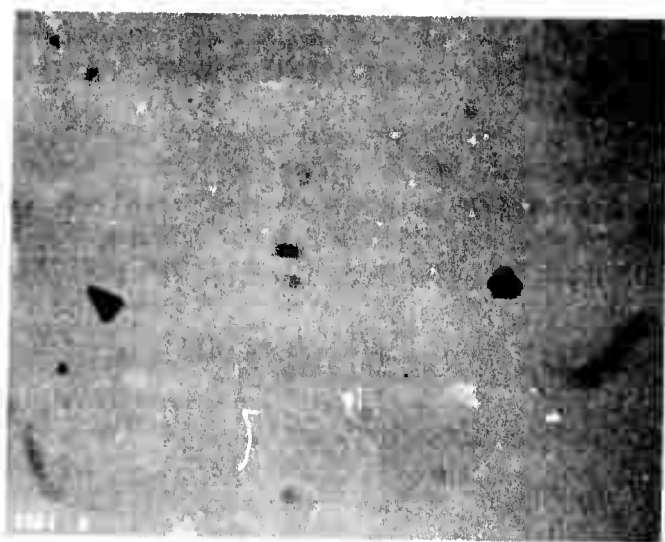
a) Iridium Inclusions (200X)
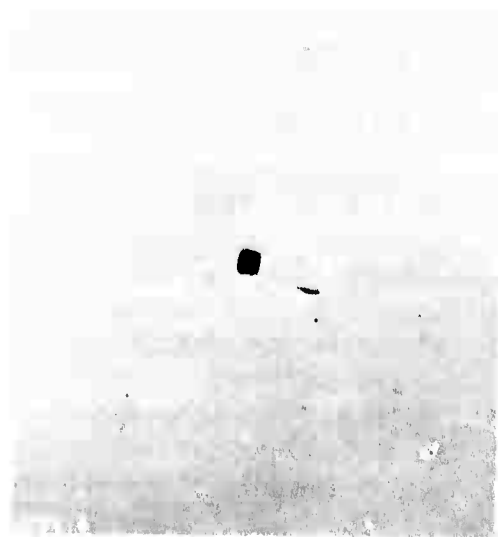
b) Gadolinium Gallium Suboxide Particle (1000X)

Figure 4. Common Inclusions in $Gd_3 Ga_5 O_{12}$

melts to become non-stoichiometric with time and for the last part of the crystal to contain a very high density of inclusions. That portion of the crystal is removed before the crystal is evaluated.

2.3.4 Dislocations

Dislocations have not been a serious problem for crystals grown in the better insulated furnace (except for those grown at high rotation rates). Experience indicates that dislocations can be introduced by sudden, large changes in temperature during growth which cause rapid changes in the crystal diameter. Therefore, efforts are made to minimize temperature changes and to grow crystals with uniform diameter.

2.3.5 Lattice Constant

The lattice constants of the crystals are listed in Tables II and III. For some crystals the lattice constant was determined from near the front and also from near the rear of the crystal. In most cases, these data indicate a slightly larger lattice constant near the rear of the crystal. This is consistent with the melts changing stoichiometry as the crystal growth run proceeds. Brandle, et al[Ref. 7] have related the lattice constants of $Gd_3 Ga_5 O_{12}$ crystals to the stoichiometry of the melts from which they were grown. The lattice constant of the crystals was found to decrease with increasing excess Ga_2O_3 in the melt and to increase with increasing excess Gd_2O_3. Thus, the lattice constant data in Tables II and III suggest that Ga_2O_3 is lost from the melt as the run progresses.

The average lattice constant of the pure $Gd_3Ga_5O_{12}$ crystals grown is 12.3832 Å. This value is in excellent agreement with other recently reported data (see for example Ref. 7 and Ref. 8). It will be noted that crystal 4417 had a lattice constant of 12.3871Å. This crystal, and 4425, were grown from a crucible which had been contaminated with iron and iron was found in both of these crystals by qualitative emission spectroscopy.

2.3.6 Evaluation of Crystals from Outside Sources

During the course of this program, a limited number of $Gd_3Ga_5O_{12}$ crystals were obtained from outside sources for use and evaluation. The properties of these crystals are listed in Table IV. It will be noted that the crystal from Union Carbide was core free but had a high defect density. This is in agreement with the results reported here. However, both Union Carbide and Airtron recently have announced core-free $Gd_3Ga_5O_{12}$ with defect densities of less than 20 cm^{-2}. This development should have a significant impact on the perfection of epitaxial films grown on such substrates.

2.4 Conclusions

Crystals of $Gd_3Ga_5O_{12}$ can now be grown essentially free of all defects which might introduce pinning sites in epitaxial films of the magnetic garnets. Although the "best" crystals often exhibit a core and growth striations, recent advances in the technology offer promise of core-free, dislocation-free crystals in the near future. Indeed, such crystals are already available in diameters up to about 3/4 inch. High

quality crystals and substrates are now available from at least two
commercial sources: Airtron and Union Carbide. It is expected that
additional commercial sources will be announced as interest in
magnetic bubble technology grows.

TABLE IV

Crystals From Outside Sources

Crystal	Lattice Constant Å	Remarks
Crystal Technology - 1	12. 3826	Defect Density $< 10^2 cm^{-2}$ - core and striations
Union Carbide - 2	12. 3838	Defect Density $> 10^4 cm^{-2}$ - core free
Airtron - 2	12. 3780	Defect Density $< 10^2 cm^{-2}$ - core and striations
Airtron - 3	12. 3834	Defect Density $< 10 cm^{-2}$ - core and striations

3.   SUBSTRATE PREPARATION

A uniform, low coercivity epitaxial magnetic film requires a nearly perfect, exceptionally clean substrate surface. Many of the defects found in present day epitaxial garnet films can be traced directly to remnant work damage from inadequate lapping and polishing of the substrate. The importance of proper substrate preparation cannot be emphasized too strongly.

Monsanto has maintained a continued interest in the surface preparation of garnet substrates since the inception of its magnetic oxide program. It has drawn upon its extensive experience in the preparation of silicon and III-V semiconductor surfaces to develop methods of preparing garnet surfaces. As a result it has developed a combined mechanical/ chemical process using Syton as a final polishing step which produces a high quality surface suitable for epitaxial growth for both LPE and CVD methods. It is not clear how Syton polishes garnet but it is believed that both a chemical and mechanical action is involved. Since substrate preparation is so important, this process is described here in detail.

Wafers of nominal 20 mil thickness are sliced from an oriented $Gd_3 Ga_5 O_{12}$ crystal with a diamond impregnated OD saw. The wafers are cleaned and cemented onto a stainless steel lapping block using a minimum of Carnauba wax. The wafers are then lapped to the same thickness on a Lapmaster* machine equipped with a cast iron lapping plate; $3 \mu Al_2O_3$

---

* Lapmaster is a trade name of the Crane Packing Co.

suspended in a mixture of deionized water and glycercine is used as the abrasive.

The wafers are then demounted and turned over on the lapping block. Again a minimum of Carnauba wax is used to cement the wafers and all excess wax is carefully removed from the wafers and lapping block. The wafers are again lapped on the Lapmaster, using $3 \mu Al_2O_3$ until at least two mils of material are removed. The wafers and block are then scrubbed with warm soapy water and a nylon brush, soaked in warm soapy water in an ultrasonic cleaner and finally rinsed in deionized water.

Another two mils are then removed from the surface on a Robinson-Houchin polisher using $0.3 \mu Al_2O_3$ and a AB Texmet* polishing lap. The wafers and block are again thoroughly cleaned in warm soapy water.

Finally an additional mil of surface is removed on a Syton** flooded Corfam*** lap. The Syton is diluted with deionized water - 20 parts Syton, 15 parts water. The final thickness of the wafers is about 13-15 mils.

After demounting, the wafers are rinsed three times in boiling trichloroethylene, then once in boiling isopropyl alcohol and dried in a stream of filtered nitrogen. To ensure that all traces of Syton have been removed, the wafers are then soaked for 10 seconds in concentrated HF.

---

*   Texmet is a trade name of Buehler Ltd.
**   Syton is a trade name of Monsanto Co.
***   Corfam is a trade name of Dupont

After rinsing in deionized water and drying in hot isopropyl alcohol the wafers are mounted in a Teflon rack and given a final cleaning:

1. 5 minute soak in each of two beakers of warm (50°C) H_2SO_4

2. 3 rinses in deionized H_2O

3. 1 rinse in hot isopropyl alcohol in an ultrasonic cleaner

4. 1 rinse in hot isopropyl alcohol

5. Dried in a stream of filtered N_2.

(The sulfuric acid and solvents used in the cleaning procedure are Transitar grade obtained from Mallinckrodt Chemical Works). Good housekeeping habits and cleanliness cannot be over-stressed in the polishing and cleaning procedures.

Recently it was determined that the intermediate lapping with 0.3μ Al_2O_3 could be eliminated if an extra 1/2 to 1 mil of material were removed on the Syton lap.

These procedures have been found to produce excellent surfaces for the growth of epitaxial garnet films by either LPE or CVD. Etching in hot orthophosphoric acid at 160 - 170°C reveals no scratches or residual work damage. However, the Syton polishing does result in considerable rounding of the edges of the wafers. Other polishing methods have been investigated in an effort to preserve the flatness of the wafers. These have included polishing with diamond on a tin lap, and with Syton on both a Teflon and polyurethane lap. Although flatness was preserved by these methods, the resulting surfaces were not free of work damage. Experience indicates that residual work damage on the surface of wafers to be used for

epitaxial deposition cannot be tolerated.

Satisfactory surfaces have also been obtained by chemically polishing the wafers in orthophosphoric acid at about 300°C. However, it is difficult to obtain reproducible results with this polish and it appears to offer no real advantage over the chemical/mechanical method described above.

4. LIQUID HASE EPITAXY

4.1 Introduction

Liquid phase epitaxy (LPE) of garnets involves the growth of magnetic layers on non-magnetic garnet substrates from a molten oxide solution in which an appropriate amount of magnetic garnet of the desired composition has been dissolved. Solvent systems from which garnet films have been grown include $PbO-B_2O_3$[Ref. 9], $BaO-B_2O_3$[Ref. 10], and $Bi_2O_3-V_2O_5$[Ref. 11]. The best results reported to date have been obtained with the $PbO-B_2O_3$ solvent, and this is the one primarily used in this work. However, the use of the BaO-based solvent was investigated also.

There are two basically similar LPE techniques by which garnet films are commonly grown. One, known as the "tipping" technique, involves pouring the garnet solution over the substrate and cooling for a prescribed length of time, and the other, known as the "dipping" technique, involves dipping the substrate into the garnet solution for a prescribed length of time. The second technique, because of its relative speed, convenience and capability for achieving reproducibility is the one being used at Monsanto.

Several magnetic garnet film compositions possessing desirable properties for magnetic bubble devices had been grown at Monsanto by the dipping process before this program was initiated, and most of the experimental details and procedures were well established. This familarity with the processes involved enabled Monsanto to prepare and deliver five completely characterized and nearly identical films of each of six different high performance magnetic garnet compositions in a relatively short period

of time. Essentially, this work involved the adjustment of solution composition to yield epitaxial films possessing the desired magnetic properties. This task was not a trivial one and required the closest cooperation and liason between the analytical and characterization groups and the crystal growers. The rapid feed-back of information on the properties of exploratory compositions was essential to the success of this program.

4.2   Experimental

4.2.1   LPE Dipping Station

Figure 5 is a schematic drawing of an LPE dipping station. The relatively simple apparatus consists of a Kanthal wound, resistance tube furnace mounted vertically. A close-fitting, heavy wall (1/4 inch) alumina tube is used to line the bore of the furnace. The liner serves primarily to protect the furnace windings from corrosive fumes. In the past, the furnace bore has been lined with platinum and various platinum baffles were used to distribute the heat uniformly in the hot zone. However, equally satisfactory results were obtained with the arrangement illustrated here. A 30ml platinum crucible is supported on a firebrick pedestal slightly below the hottest zone of the furnace. The temperature is controlled with a Pt vs Pt - 13% Rh thermocouple placed against the alumina liner. A second Pt vs. Pt - 13% Rh thermocouple is used to monitor the solution temperature. This thermocouple abuts the Pt crucible.

The substrate is mounted in a Pt wire holder which is attached to an alumina rod. The rod and substrate are moved in and out of the furnace by means of a lab jack. Before the substrate is immersed in the solution
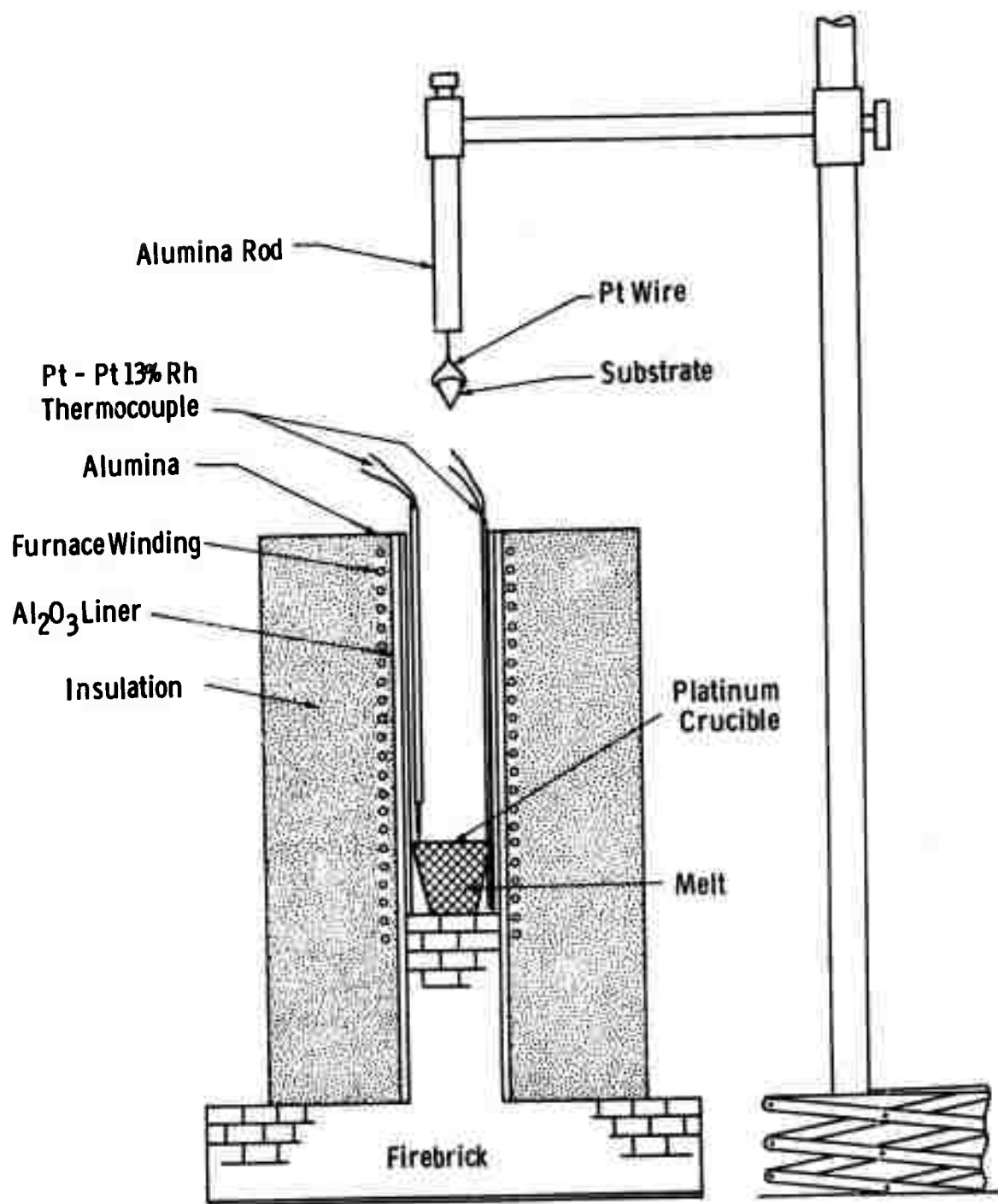
29

Figure 5. Schematic of LPE Dipping Station

it is held just above the melt surface for about 10 minutes to allow the substrate temperature to reach the solution temperature. The substrate is then dipped into the solution for a prescribed length of time during which film growth occurs. To ensure film thickness uniformity, the substrate is tilted in its holder to conform approximately with an isotherm in the solution. After the prescribed growth time, the substrate is raised from the melt whereupon the flux drains off and the substrate plus epitaxial layer can be removed from the furnace.

4.2.2 Materials

The rare earth oxides used in this work were obtained from Lindsay Rare Earths and were of 99.99 percent purity; Fe_2O_3 of 99.9 percent purity was obtained from Ventron-Alfa Inorganic and Ga_2O_3 of 99.99 percent purity was obtained from Alussise. Both Grade I and Grade II PbO, obtained from United Mineral and Chemical Corp. were used. No significant difference in results were noted between these grades of PbO. B_2O_3 of 99.99 percent purity was obtained from British Drug Houses, Ltd.

The oxides are weighed to four significant places and melted together in the 30 ml Pt crucible. The solution is homogenized at about 1050°C, well above the liquidus temperature of the compositions used, for 2 to 4 hours before being cooled to growth temperatures.

4.3 Results and Discussion

4.3.1 The PbO-B_2O_3 Solvent System

Lead oxide based fluxes have been used extensively as solvents from which to grow rare earth magnetic garnet crystals. (See, for example, Ref. 12 and Ref. 13). The PbO-B_2O_3 system, composed of 50 parts PbO to 1 part B_2O_3 (by weight), was chosen as the primary solvent to be used in this work. This is the solvent system used by Schick, et al[Ref. 9] and Levinstein et al[Ref. 11 and Ref. 14] for the epitaxial growth of garnet films. It has been used extensively at Monsanto and elsewhere with consistently good results for a wide variety of complex magnetic garnet compositions.

The rare-earth magnetic garnets are incongruently saturating in the chosen solvent as they a   in all PbO-based solvents. The phase relationships in these systems require that the solution contain an excess of Fe_2O_3 (over that required by the garnet formula) in order to maintain the system in the garnet stability region. Too little Fe_2O_3 places the system in the orthoferrite stability region where, at growth temperatures in the range 800°C to 1000°C, an orthoferrite phase can precipitate on the surface of the melt. Garnet films grown from a solution which is too near the orthoferrite phase invariably display well developed etch pits. Too much Fe_2O_3 places the system in the magnetoplumbite stability range. Solutions containing from 10 to 14 times as much Fe_2O_3 as rare-earth oxide (by mole percent) have been found to be satisfactory for the deposition of high quality magnetic garnet films having smooth, uniform surfaces and

substrate-film interfaces free from excessive attack and interdiffusion.

The solubility of garnet in the $PbO-B_2O_3$ solvent is not well known. Accurate measurements are difficult to make in any such multicomponent systems, and, in this case, are complicated by loss of PbO by evaporation! However, some practical solubility data have been accumulated at Monsanto for a number of solution systems of interest. The liquidus temperatures were established by observing, repeatedly, the temperature at which the last solids dissolved as a well-stirred, two phase mixture was slowly heated. The liquidus temperatures thus found depend upon total solute concentration and are given for specific solution systems in Appendix B.

It was found that the rare-earth oxides are only sparingly soluble in the $PbO-B_2O_3$ solvent. In all cases studied, the solubility of the rare-earth oxides was less than one mole percent over the temperature range investigated (about 850 to 1000°C). For this temperature range, the garnet stability range is indicated on the ternary phase diagram shown in Figure 6.

It has proven possible to super-cool the melt by over 100°C for solutions sufficiently dilute in garnet, and to maintain the solution in the supersaturated state for several days. Under these conditions garnet films can be grown at constant temperature, the film thickness being determined only by the degree of supersaturation and the time the substrate remains in the melt. This is a very desirable situation and quite significant from the standpoint of reproducibility.
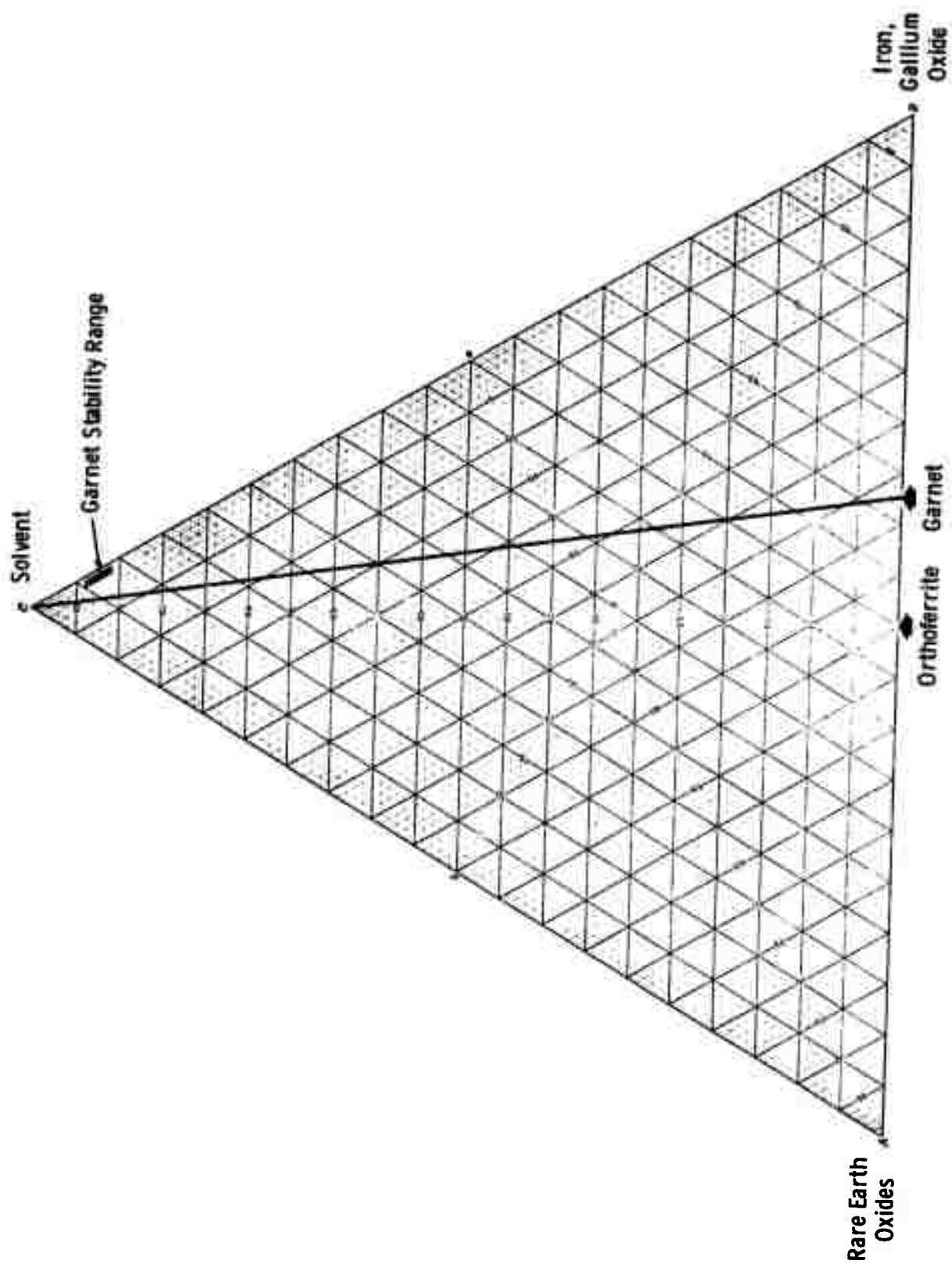
Figure 6. Ternary Phase Diagram Showing Garnet Stability Range

The best, most consistent results have been obtained with super-cooling of about 30 to 40°C. At larger degrees of supercooling smooth films are usually not obtained. In addition, spurious nucleation and precipitation of solids on the melt surface often occurs when the solution is disturbed at higher degrees of supercooling.

Within the preferred range of (supercooling (30° - 40°C)) the film growth rates vary from about 0.2 μm/min to about 0.4 μm/min for the films grown during this program. However, it was observed that film growth rates decrease with time as the supercooled solution is left undisturbed at growth temperature. This behavior is illustrated by the data of Table V. These data were collected by growing epitaxial layers at various times after the solutions had been homogenized at about 1050°C (well above the liquidus temperature in each case), stirred, and cooled to growth temperature. The solutions were left undisturbed except for immersing and withdrawing the substrate. Each solution was supercooled about 30 to 40°C and in no case did precipitation occur during the course of the experiments. In every case, the film growth rate decreased with time as the melt was left undisturbed. The greatest decrease occurred in the first few hours after the solution had been cooled from homogenization temperature to growth temperature.

After Sample No. 4485C (Table III) was grown, the solution was stirred vigorously at growth temperature and another film (4485D) was grown. The growth rate was low. The solution was then reheated to 1050°C

TABLE V

Decrease of Film Growth Rate With time In Undisturbed Solutions

Nominal Composition	Sample Number	Growth Temp. (°C)	Time at Temp. (hrs)	Growth Rate (μm/min)
$Eu_{0.70}Eu_{2.3}Fe_{4.3}Ga_{0.7}O_{12}$	4421 A	885	1.25	0.167
"	4421 B	885	2.50	0.119
"	4421 C	885	22.0	0.077
"	4421 D	885	25.0	0.064
$Gd_{0.8}Er_{2.2}Fe_{4.5}Ga_{0.5}O_{12}$	4446 G	904	2.0	0.213
"	4446 H	904	3.0	0.130
"	4446 I	904	5.0	0.126
"	4446 J	904	24.0	0.110
$Gd_{0.45}Y_{2.55}Fe_{4.0}Ga_{1.0}O_{12}$	4485 A	968	0.5	0.535
"	4485 B	968	24.0	0.109
"	4485 C	968	48.0	0.087
"	4485 D*	968	---	0.007
"	4485 E*	968	---	0.60

* See Text

and maintained at that temperature for one hour <u>without</u> stirring or being disturbed. The solution was then cooled to growth temperature (968°C) and another film (4485E) was grown - the original growth rate was recovered!

These results were unexpected and are not understood. One explanation might be that an association of solution components occurs in the supercooled solutions. The decrease of growth rate with time indicates that the degree of supersaturation is becoming less with time. Since precipitation does not occur, this suggests that some sort of ionic or molecular ordering or association might be taking place so that garnet is not readily available for precipitation. Stirring the melt at growth temperatures is not sufficient to break up these complexes and restore the growth rate; however, when the solution is reheated above the liquidus, the association is destroyed and the solution can again be supercooled and growth rates restored. A slow association of solution components with time could also account for the remarkable stability of these supercooled solutions. However, it must be emphasized that, as yet, there is no direct evidence of any sort of association taking place in the solutions. Indeed, there is no clear idea of what type of association might be likely to take place.

The decrease of growth rate with time must be taken into account when it is desired to grow a series of films of the same thickness. To ensure reproducibility the films must be grown at approximately the same length of time after the solution has been cooled to growth temperature.

In this work, in order to reproduce growth rates, solutions were homogenized by maintaining the melts at about 1050°C for one to two hours. The solutions were stirred occasionally while at this temperature. The solutions were then quickly cooled to the predetermined growth temperature and the substrates were immersed 60-70 minutes after the melts reached growth temperature.

LPE mixed garnet films do not contain the rare earth ions in the same proportion as they are present in the solution. The segregation coefficients of the ions have been found to depend upon the relative size of the ions present in solution. In addition, although the iron-gallium concentrations are determined primarily by the Fe_2O_3/Ga_2O_3 mole ratio in solution, there is also a dependence on growth temperature. Less gallium substitutes for iron in the growing layer at low growth temperatures than at high temperatures. Since the composition of the film affects the magnetic properties as well as physical properties (such as the film lattice constant) an empirical iteration between the composition of the melt and the growth temperature is necessary in order to produce a magnetic garnet film having the desired composition, magnetic properties, and structural quality. The segregation coefficients of the solutes are discussed in more detail later in this report in relation to specific solution systems.

There is generally some incorporation of the solvent constituents into the growing layer; not as inclusions, but substitutionally. Particularly at low growth temperatures, enough Pb^{2+} substitutes into rare-earth sites

and induces Fe^{4+} that the layers take on a decidely reddish cast. The incorporation of Pb is strongly temperature dependent. For example, A $Eu_1 Er_2 Ga_{0.6} Fe_{4.4} O_{12}$ film grown from a solution at 850°C had a Pb concentration of 2.5 weight percent (by electron microprobe analysis). Another film, grown from the same solution at 900°C, contained less than 0.5 weight percent lead. The approximate dependence of Pb incorporation on temperature is shown in Fig. 7 which also includes some data from IBM [Ref. 15] and Hewlett-Packard [Ref. 16]. The scatter in the data probably results from Pb incorporation having a dependence on growth rate, as well as on temperature.

The saturation magnetization and Neel temperature of Pb-containing layers is generally less than that of Pb-free layers of the same composition. As yet, it is not clear if Pb affects the dynamic properties of the film. In any case, as the data of Fig. 7 suggests, Pb contamination can be minimized by epitaxial growth above 900°C. Most of the films grown on this program were grown at temperatures above 900°C and are essentially Pb free as determined by electron probe microanalysis.

4.3.2 The Eu-Er Magnetic Garnets

The Eu-Er magnetic garnets were among the first of the mixed and substituted garnets which were discovered to exhibit uniaxial magnetic anisotropy [Ref. 17]. These garnets exhibit "growth-induced" anisotropy which is believed to arise from a preferential occupation of the dodecahedral
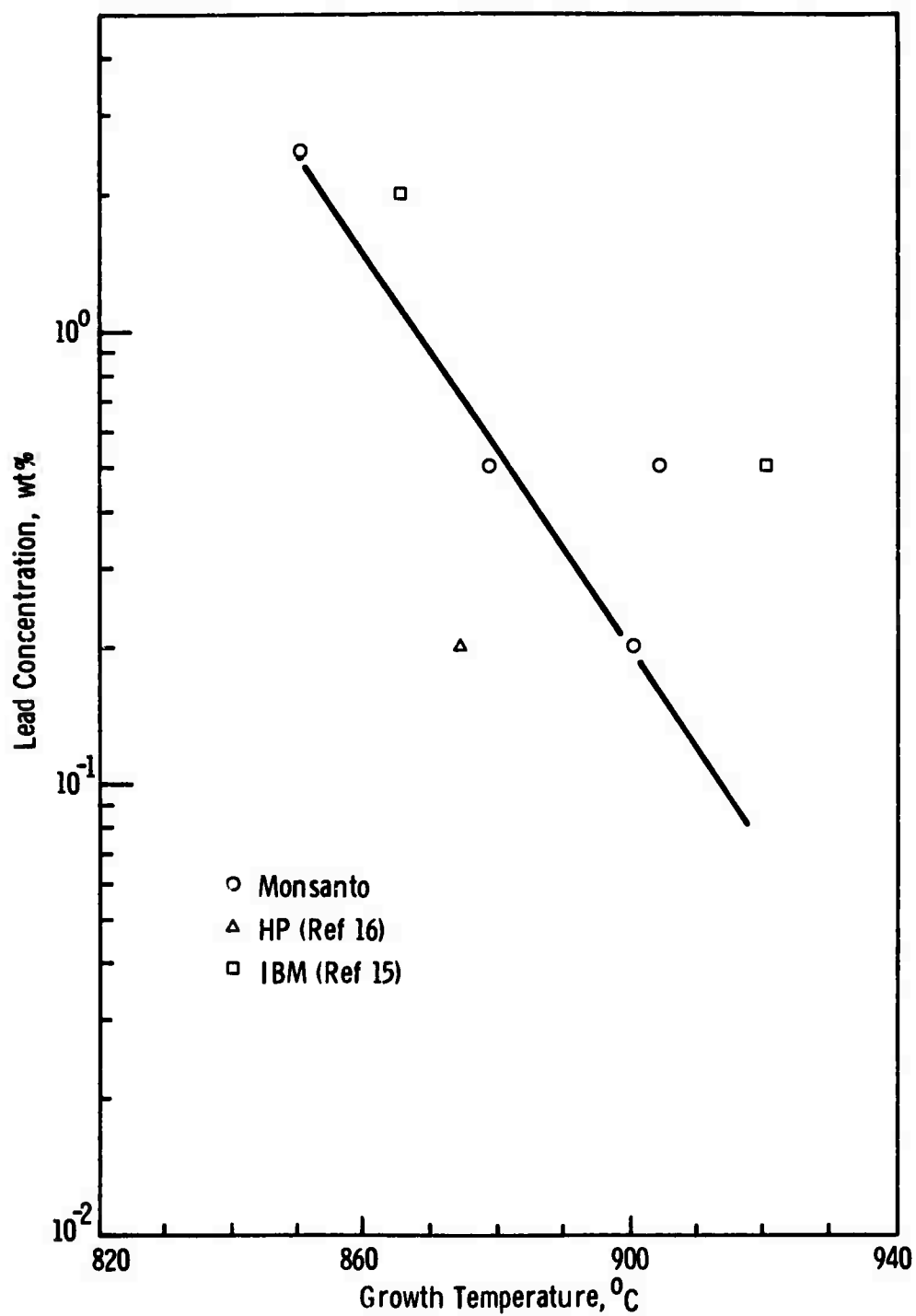
Figure 7. Lead Concentration in Super IV^{-1} Films as a Function of Growth Temperature

sites by the two rare-earth ions. Following the nomenclature of the workers at Bell Telephone Lab. the $Eu_2 Er_1 Fe_{5-x} Ga_x O_{12}$ compositions are designated as Super IV and the $Eu_1 Er_2 Fe_{5-x} Ga_x O_{12}$ compositions are designated as Super IV^{-1}. The term "Super" as used here refers to the non-cubic magnetic superstructure associated with the usual cubic anisotropy of the garnets.

The lattice constants of the Super IV^{-1} compositions containing an appropriately adjusted Eu/Er ratio and Fe/Ga ratio have a good match to $Gd_3 Ga_5 O_{12}$ — the most readily available of the non-magnetic candidate substrate materials. In addition Super IV and Super IV^{-1} were the first magnetic garnets which exhibited growth-induced anisotropy to be grown as epitaxial films by LPE[Ref. 9]. Consequently, these compositions received the principal interest in the early LPE work, both at Monsanto and in the industry in general. Super IV^{-1}, deposited on $Gd_3 Ga_5 O_{12}$ substrates, was chosen to be the first material to be supplied to ARPA on this program.

Because of the early work, both at Monsanto and elsewhere, considerable information concerning the LPE growth of Super IV^{-1} of predetermined magnetic properties had been accumulated before work on this program began. Solution compositions, growth temperatures, etc., were generally well known.

In order to prepare a solution to yield a film of predetermined composition , it is necessary to know the segregation coefficients of the

41

film components, the rare earths, iron and gallium. For this, it is convenient to define segregation coefficients in the following terms:

$$\alpha_{RE} = \frac{\left[\dfrac{C_{RE}}{\Sigma C_{RE}}\right]_{film}}{\left[\dfrac{C_{RE}}{\Sigma C_{RE}}\right]_{solution}} \quad \text{and} \quad \alpha_{Ga} = \frac{\left[\dfrac{C_{Ga}}{C_{Ga} + C_{Fe}}\right]_{film}}{\left[\dfrac{C_{Ga}}{C_{Ga} + C_{Fe}}\right]_{solution}}$$

where α_{RE} is the segregation coefficient of a particular rare earth, C_{RE} is the mole fraction of the rare earth and ΣC_{RE} is the sum of the mole fractions of all rare earths involved. Analogous definitions apply to the segregation coefficient of gallium, α_{Ga}, and of iron α_{Fe}.

For the Super IV^{-1} composition, the segregation coefficients of Eu and Er were found to be 1.04 and 0.98, respectively. (Film compositions were determined by electron probe microanalysis). These coefficients did not appear to depend upon growth temperature. This is not the case for gallium, however. The segregation coefficient of gallium increased from about 1.68 at a growth temperature of 878°C to 2.17 at a growth temperature of 952°C as shown in Fig. 8.

The principal problem associated with the preparation of Super IV^{-1} is to obtain films of low coercivity. The anisotropy field of Super IV^{-1} is about 5000 Oe. Such a high anisotropy leads to very narrow domain walls. Narrow walls interact strongly with even small defects in the film or at the film/substrate interface to result in high coercivity. For high anisotropy materials, films must be of high perfection to achieve low coercivities.
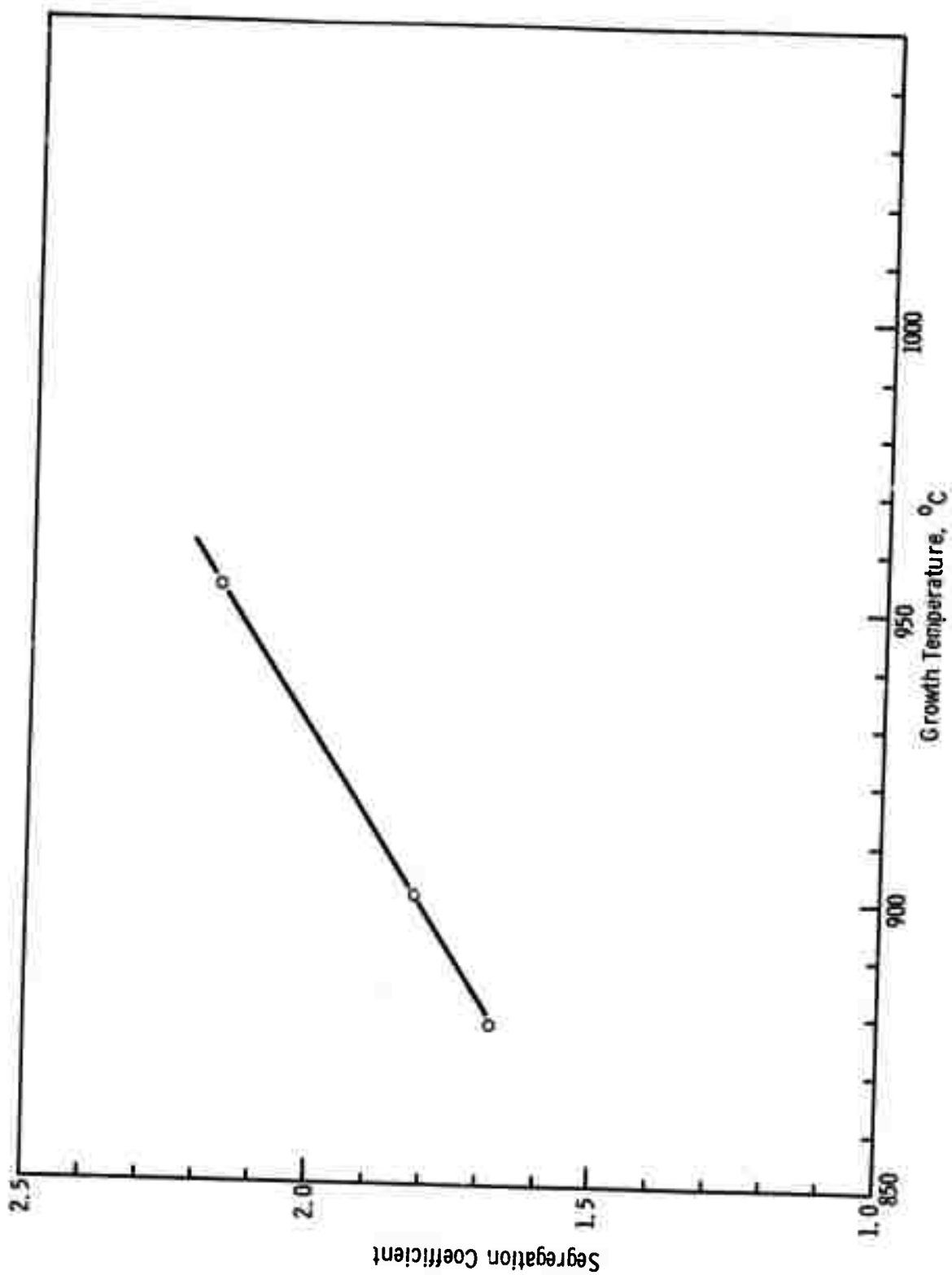
Figure 8. Segregation Coefficient of Gallium as a Function of Film Growth Temperatures for the Super IV⁻] Garnets

In the case of Super IV^{-1}, it was found that a very close match between film and substrate lattice constant was necessary to achieve low coercivity. It is possible to calculate a reasonably accurate lattice constant for a film composition by using published values of lattice constants of the end members (iron and gallium garnets) and assuming Vegard's law. In addition, Giess et al[Ref. 15] have shown that Pb ion incorporation increases the lattice constant of the film composition by 0.013Å per weight percent Pb present. Therefore, the lattice constants, a_0, of the $Eu_y Er_{3-y} Fe_{3-x} Ga_x O_{12}$ garnets can be estimated from the expression:

$$a_0 = 12.349 + 0.0497y - 0.015 x + 0.013Pb$$

where Pb is the weight percent Pb present in the layer.

The importance of matching film lattice constant to that of the substrate to achieve low coercivity in the Super IV^{-1} compositions is illustrated by the data in Table VI. Here are tabulated the range of coercivities measured on a number of films of the indicated compositions. These films were grown on $Gd_3 Ga_5 O_{12}$ substrates with a lattice constant of 12.378Å. The films contained about 0.5 weight percent Pb. The lattice mismatch is the difference:

$$a_0 \text{ (substrate)} - a_0 \text{ (film)}.$$

The coercivities, 0.1 to 0.5 Oe, found for the $Eu_{0.63} Er_{2.37} Fe_{4.3} Ga_{0.7} O_{12}$ composition, compare favorably with the lowest reported for Super IV^{-1} films on $Gd_3 Ga_5 O_{12}$ and, evidently, represent the practical lower limit of coercivity which can be obtained for this garnet system. This is the

TABLE VI

Lattice Constant and Coercivities for Some Super IV^{-1} Compositions

Nominal Composition	Pb Conc. (w/o)	Estimated Lattice Constant* (Å)	Lattice Constant Mismatch (Å)	Coercivity (Oe)
$Eu_1Er_{2.0}Fe_{4.3}Ga_{0.7}O_{12}$	0.5	12.395	-0.018	1 - 5
$Eu_{0.84}Er_{2.16}Fe_{4.3}Ga_{0.7}O_{12}$	0.5	12.387	-0.009	1 - 2
$Eu_{0.62}Er_{2.38}Fe_{4.3}Ga_{0.7}O_{12}$	0.5	12.376	+0.002	0.1 - 0.5
$Eu_{0.55}Er_{2.45}Ga_{4.3}O_{0.7}O_{12}$	0.5	12.370	+0.008	> 1
$(Gd_3 Ga_5 O_{12}$	- .-	12.378	Substrate	-------)

* Estimated using Vegard's law.

nominal composition grown for ARPA. The solution composition and growth conditions for these films are summarized in Appendix A-1.

The Neel temperature of a number of Super IV^{-1} samples were measured during the course of this work. The Neel temperature for some Pb-free samples is plotted as a function of gallium content for a limited range of gallium concentrations in Fig. 9. The curve has been extrapolated to values obtained by averaging the Neel temperature of the pure iron garnets (see Appendix A). These data can prove valuable in estimating the gallium content of samples whose exact composition is unknown. For Pb-free samples, the gallium contents determined from Fig. 9 were in excellent agreement with that obtained by electron probe microanalysis. However, the curve could not be used for samples which contained Pb. It was found that the Neel temperature decreased with increasing Pb contamination.

4.3.3 The Gd-Er Magnetic Garnets

The Gd-Er magnetic garnets comprise another system which exhibits growth induced anisotropy. These garnets are sometimes referred to as the Super VIII garnets, the term "Super" again relating to the magnetic superstructure which results in the uniaxiality of the garnets. As in the case of the Super IV^{-1} family, the unique axis in this system is perpendicular to the (111) plane with certain Gd/Er and Ga/Fe ratios. Certain of the compositions (approximately $Gd_1 Er_2 Fe_{4.5} Ga_{0.5} O_{12}$) have lattice constants which are compatible with $Gd_3 Ga_5 O_{12}$ and these garnets can be deposited epitaxially on (111) $Gd_3 Ga_5 O_{12}$ substrates.
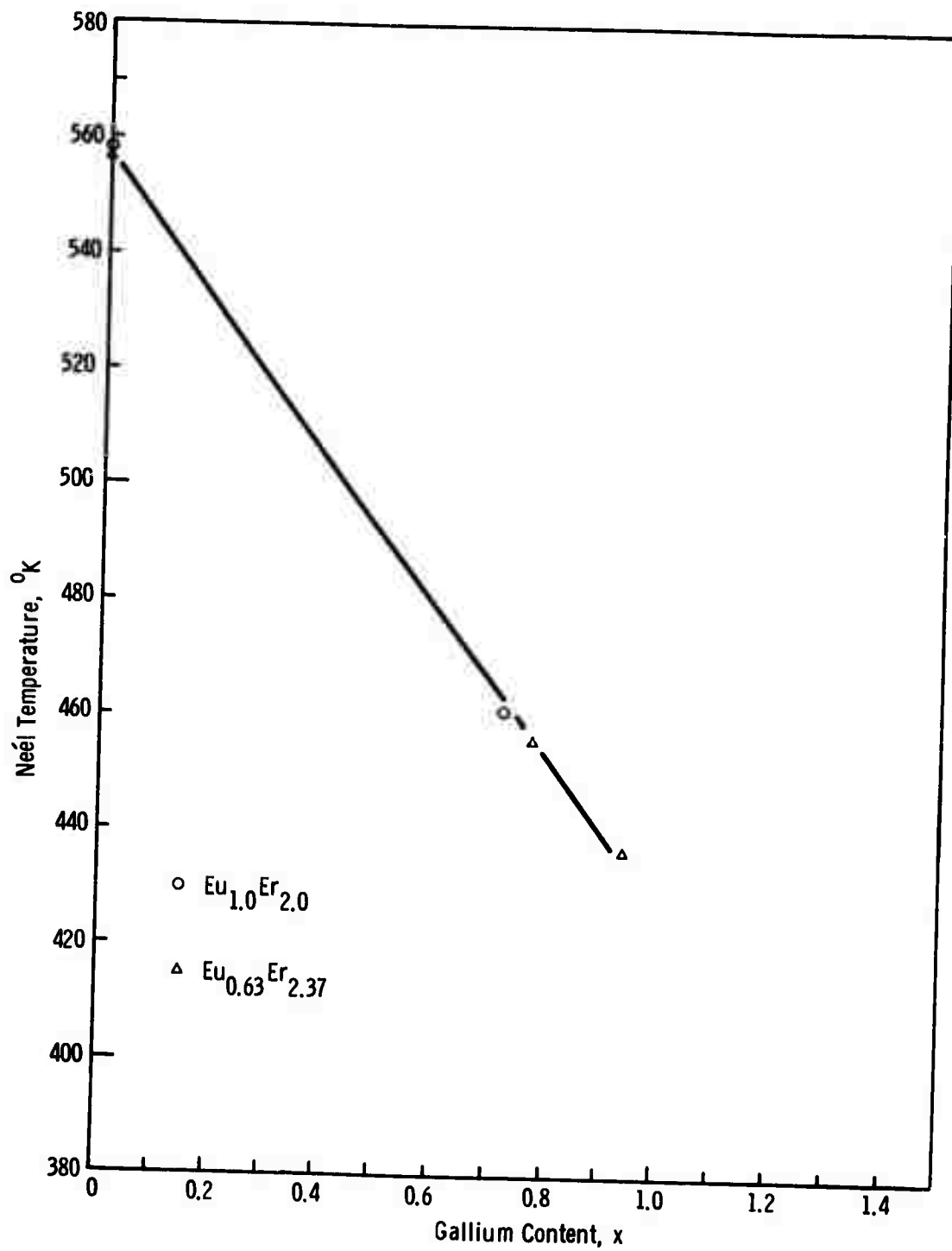
Figure 9.   Neél Temperature as a Function of Gallium Content for LPE Super IV^{-1} Garnets

47

The anisotropy of the Super VIII garnets (about 1400 Oe) is considerably less than that of the Super IV^{-1} family. Consequently, preparing films of low coercivity is not a serious problem for these garnets and coercivities less than 0.1 Oe are readily achieved. The prime problem in the growth of Super VIII was to establish the proper solution composition and growth temperature that would yield films having the desired magnetic properties (saturation magnetization, bubble size, etc.)

A number of films were grown at 900°C from $PbO-B_2O_3$ solutions containing a Gd/Er mole ratio of 1/2 and various Ga/Fe mole ratios. Substrates were wafers of (111) $Gd_3 Ga_5 O_{12}$ with a lattice constant of 12.383. The compositions of certain of the films were determined by electron probe microanalysis. Using these data and the known solution compositions the following segregation coefficients were calculated:

$$\alpha_{Gd} \quad 1.10$$

$$\alpha_{Er} \quad 0.96$$

$$\alpha_{Ga} \quad 1.74$$

It should be emphasized that these data refer to epitaxial growth at 900°C. It has already been pointed out that the segregation coefficient of gallium increases with temperature. These segregation coefficients were used to calculate the compositions of all the Gd-Er films grown at 900°C. Since the segregation coefficients of Gd and Er were not exactly unity, the epitaxial films contained slightly more Gd and slightly less Er than the solutions.

The Neel temperatures of the magnetic films were measured. In some cases, it was possible to detect a compensation temperature in addition to the Neel temperature. These data are plotted in Fig. 10 as a function of gallium content. It will be noted that the compensation temperature is above room temperature for films with gallium content, x, of about 0.57 or 0.6. The Neel temperature is extrapolated to the value of the gallium-free garnet obtained by taking a weighted average of the pure iron garnets (Appendix A).

The room temperature saturation magnetization is plotted as a function of gallium content in Fig. 11. The saturation magnetization has been found to depend on film thickness[Ref. 18] as well as composition. Since these films were of different thicknesses the points in Fig. 11 are somewhat scattered. The saturation magnetization value for the gallium-free garnets was taken as the weighted average of the pure iron garnets (Appendix A). The gallium content, 0.57, at which the compensation temperature is at 300°K was taken from Fig. 10. These two points were used to establish the saturation magnetization of the garnets with compensation temperatures below room temperature and must be regarded as approximate.

Some other pertinent properties of the $Gd_y Er_{3-y} Fe_{5-x} Ga_x O_{12}$ garnets are summarized in Table VII. A number of films of each series were prepared and the property values in the table represent an average of the values measured. The lattice constants of these films were estimated from an expression analogous to that used for the Eu-Er garnets:

49
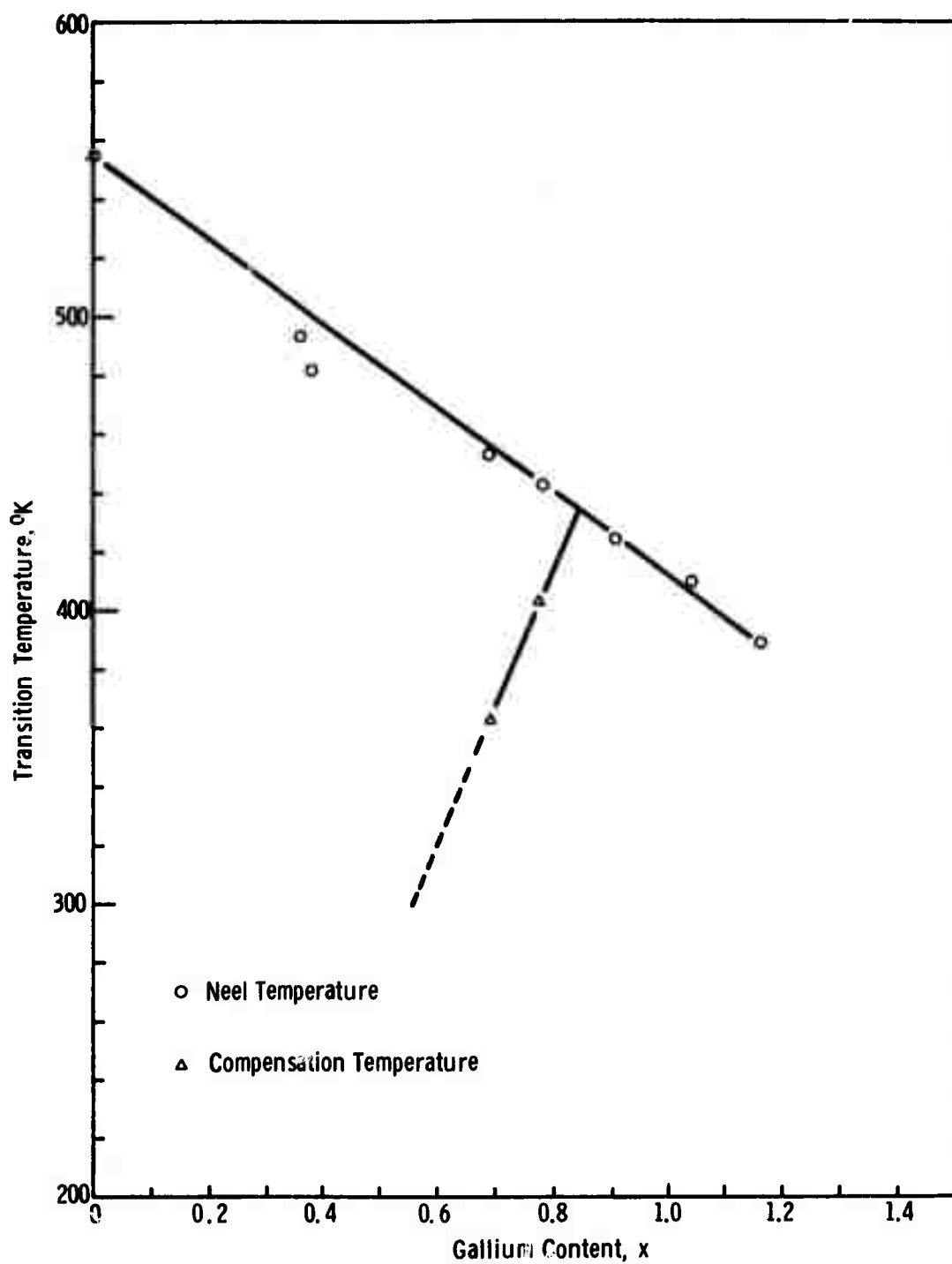
Figure 10.   Transition Temperatures as a Function of Gallium
Content for LPE Super VIII Garnets
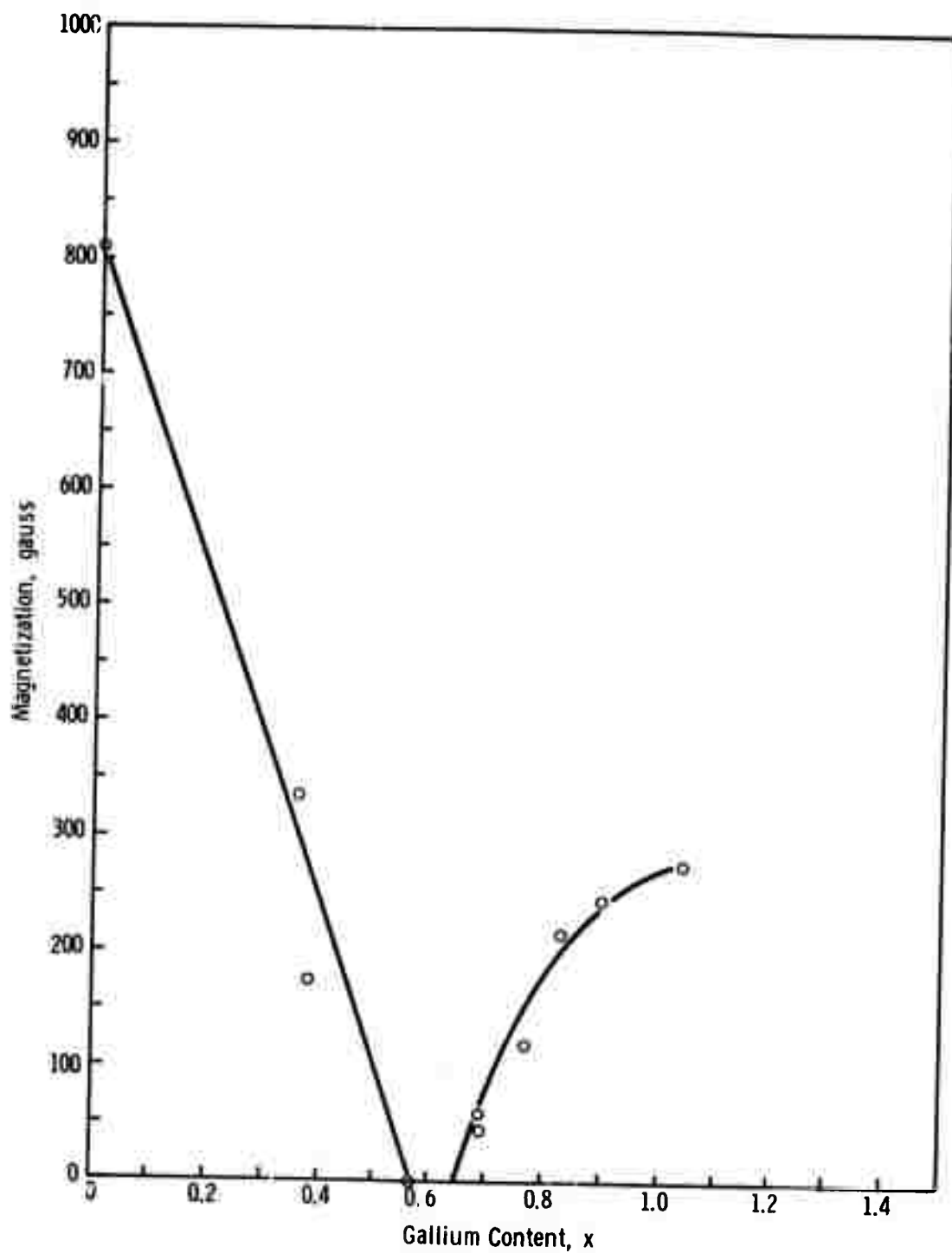
Figure 11. Room Temperature Saturation Magnetization as a
Function of Gallium Content for LPE Super VIII Garnets

TABLE VII

Properties of LPE Super VIII Garnets

Series Number	Composition	Estimated Lattice Constant (Å)	Lattice Mismatch (Å)	Coercivity (Oe)	Characteristic Length
32178	$Gd_{1.1}Er_{1.9}Fe_{4.63}Ga_{0.37}O_{12}$	12.391	+0.011	0.5	0.29
32164	$Gd_{1.1}Er_{1.9}Fe_{4.31}Ga_{0.69}O_{12}$	12.387	+0.004	0.5	1.09
32166 B	$Gd_{1.1}Er_{1.9}Fe_{4.22}Ga_{0.78}O_{12}$	12.385	+0.002	0.2	1.14
32166 D	$Gd_{1.1}Er_{1.9}Fe_{4.17}Ga_{0.83}O_{12}$	12.385	+0.002	0.2	1.14
32159	$Gd_{1.1}Er_{1.9}Fe_{3.97}Ga_{1.03}O_{12}$	12.381	-0.002	0.05	0.21
32162	$Gd_{1.1}Er_{1.9}Fe_{3.84}Ga_{1.16}O_{12}$	12.380	-0.003	0.05	--
	$Gd_3 Ga_5 O_{12}$	12.383	Substrate		

$$a_0 \overset{\circ}{} 12.349 + 0.0433y - 0.015x + 0.013Pb$$

Again, the correspondence between lattice mismatch and coercivity will be noted. The lowest coercivities were achieved with a close match between the lattice constants of film and substrate.

For temperature - insensitive magnetic properties, it is desired to have a bubble film with a compensation temperature below room temperature. In addition, bubble diameters of 5 to 6 μm are desired. These two criteria were used to select the Super VIII composition to be delivered to ARPA. The data of Figs. 10 and 11, and Table VII indicate that the nominal composition

$$Gd_1 Er_2 Fe_{4.55} Ga_{0.45} O_{12}$$
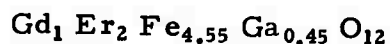
would satisfy these requirements. To ensure a close lattice match if some Pb were incorporated in the film, the Er content was increased slightly for the films grown for ARPA. The solution compositions and growth conditions for these films are given in Appendix B-2.

4.3.4 The Super V Garnets

The Super V garnets are a family of magnetic garnets based on the Gd-Y system. In this case, however, the term "Super" is somewhat misused since the anisotropy in these garnets is primarily stress-induced. Actually, the Super V garnets can be considered as derivatives of the Gd-Y garnets in which additional rare-earth ions have been substituted to enhance certain properties -- the anisotropy and temperature stability, in particular. In order to maintain the high mobility of the Gd-Y system,

rare-earth ions which exhibit little or no angular momentum are preferred for substitution. Thus, the ions Yb, Tm, Lu, La, and Eu are preferred substitutes and three of these garnets systems were prepared for ARPA.

Since the anisotropy in the Super V family is primarily stress-induced, the mismatch of substrate and film lattice constant is critical. These systems have negative magnetostriction coefficients so the films must be in tension to exhibit anisotropy perpendicular to the (111) plane. In general, it is desired to grow the film in as much tension as possible to achieve high anisotropy. However, care must be exercised to ensure that the lattice mismatch is not enough to cause the film to crack.

The lattice mismatch was found to be especially critical in the case of the Gd-Y system. Observations of magnetization and anisotropy versus Gd ion concentration of LPE films grown at 950-1000°C led to the conclusion that there was a growth-induced, in-plane anisotropy which, for films containing enough Gd, was sufficient to overcome the stress-induced anisotropy normal to the film. For as-grown films, a tolerance of only 0.003Å was found between that lattice mismatch necessary to yield bubble domains and that which caused film cracking. It was necessary to mix and equilibrate 15 different LPE garnet solutions and grow over 30 layers to solve the problem sufficiently to obtain good, device-quality films. It should be pointed out that the growth-induced in-plane anisotropy could probably be eliminated by high temperature annealing. However, it was felt that such post-growth treatment was outside the scope of this phase of

the program. In addition, it was desired to compare the properties of as-grown films belonging to the Super V family.

The high magnetostriction coefficients of Yb and Tm (-4.5 and -5.2 x 10^{-6}, respectively) help alleviate the problem of substrate/film lattice mismatch. The addition of either of these ions to Gd-Y raises the magnetostriction coefficient of the whole system so that an equivalent anisotropy can be obtained with a smaller lattice mismatch. In addition, these ions may introduce a component of growth-induced anisotropy normal to the film plane or, at least, reduce the in-plane anisotropy which is natural to the Gd-Y systems.

'his latter effect is the prime reason for introducing small amounts of L   o the Gd-Y lattice. Replacement of part of the Gd ions with the large La io.   kes it possible to formulate a Super V composition of desirable propert.   iich matches the lattice constant of $Gd_3 Ga_5 O_{12}$ without using undue amounts of Gd. Thus, the in-plane growth induced anisotropy can be minimized.

Although the lattice mismatch tolerance is not as limited for the substituted Super V garnets as in the case of the Gd-Y system, film compositions still have to be precisely adjusted to yield the desired relationship between saturation magnetization and anisotropy. Since these compositions involve one more ions than Super IV or Super VIII the adjustment is somewhat more complicated. In addition, rare-earth ion segregation coefficients significantly different from unity were found for these compositions. Thus, the

film composition differs appreciably from the solution composition in most cases. Segregation coefficients for these systems at a specified growth temperature are listed in Table VIII. In all cases, Gd enters the lattice preferentially. This is not surprising when it is realized that the compositions are being tailored to fit the $Gd_3 Ga_5 O_{12}$ lattice. However, it should be emphasized that some dissolution of the substrate takes place before epitaxial growth occurs. Thus, the apparent high segregation coefficient of Gd may be due to the reincorporation of Gd dissolved from the substrate before film growth was initiated. The segregation coefficients of the other rare earths decrease approximately in proportion to the amount by which they differ in size from the Gd ion.

The solution compositions and growth conditions for the Super V films supplied to ARPA are summarized in appendices A-3 through A-6. Some properties of these compositions (representing an average of the films supplied to ARPA) are listed in Table IX.

In Table IX, the characteristic length of the Gd-Y composition is seen to be quite small. This is a consequence of the low anisotropy achieved in this system. It is possible that some increase in characteristic length and anisotropy could be achieved by optimizing the composition; however, it is doubtful that these parameters could be increased significantly in as-grown LPE films. The sizeable component of in-plane growth-induced anisotropy needs to be destroyed by heat-treatment at elevated temperatures.

TABLE VIII

Segregation Coefficients for the Super V Garnets

System	Growth Temperature	Segregation Coefficient					
	(°C)	Gd	Y	Yb	Tm	La	Ga
Gd-Y	970	1.02	0.99	--	--	--	1.89
Gd-Y-Yb	950	1.21	0.90	0.96	--	--	1.98
Gd-Y-Tm	950	1.28	1.15	--	0.71	--	1.97
Gd-Y-La	944	1.47	1.10	--	--	0.24	1.80

TABLE IX

Properties of Some LPE Super V Garnets

Composition	Saturation Magnetization (gauss)	Characteristic Length (μm)	Anisotropy (Oe)	Wall Mobility (cm/sec-Oe)
$Gd_{0.46}Y_{2.54}Fe_{3.95}Ga_{1.05}O_{12}$	140	0.47	350	460
$Gd_{.99}Yb_{0.86}Y_{1.15}Fe_{4.16}Ga_{0.84}O_{12}$	160	0.53	610	520
$Gd_{1.09}Tm_{0.98}Y_{0.98}Fe_{4.32}Ga_{0.68}O_{12}$	160	0.72	1160	300
$Gd_{0.44}La_{0.04}Y_{2.52}Fe_{4.01}Ga_{0.99}O_{12}$	115	0.70	580	400

The characteristic length of the Gd-Yb-Y films is somewhat low also. In this case, it is felt that additional Ga could be introduced into these films. This would have the effect of both reducing the saturation magnetization and increasing the anisotropy (by decreasing the lattice constant of the film and thereby increasing the lattice mismatch and strain), and, thus, increasing the characteristic length.

Both the Gd-Tm-Y and Gd-La-Y compositions have characteristic lengths in a desirable range. These films will support stable bubbles with diameters of 5 to 6 microns.

Because of the dependence of mobility values upon pulsed field amplitude as well as their inherent uncertainty (Ref. 2), it is not entirely clear that the differences in this property listed in Table IX are significant. However, all the Super V compositions have wall mobilities exceeding 200 cm/sec Oe, a desiratum specified in the Introduction of this report.

4.3.5 The BaO-Based Solvent System

A second solvent system from which magnetic garnets have been grown is based on BaO. Linares (Ref. 18) first described the use of the $BaO-B_2O_3$ system in the preparation of $Y_3 Fe_5 O_{12}$. Laudise, et al[Ref. 19] also used this solvent for the growth of $Y_3 Fe_5 O_{12}$ on a seed. Recently, Burmeister, et al[Refs. 16 and 10] have improved this solvent system by additions of PbF_2 and have used the improved solvent for the epitaxial film growth of several compositions of magnetic garnets on $Gd_3 Ga_5 O_{12}$ substrates. It was an objective of this work to investigate the BaO-based solvents and to compare these solvents with PbO-based systems.

Although the BaO-based solvent system has not been used as extensively as the PbO-based solvent, it possesses certain desirable properties, which have been discussed by Burmeister, et al[Refs. 16 and 10] Briefly, these properties include the following:

(1) The vapor pressure is low at film growth temperatures

(2) The solvent does not react with platinum

(3) The solvent is relatively non-toxic

(4) Garnet is congruently saturating in the solvent

(5) Solvent constituents are not readily incorporated in the film.

In addition, the rare earth magnetic garnets are, in general, more soluble in the BaO-based solvents than in the PbO-based solvents.

In spite of these significant advantages, however, the high viscosity of the solvent at temperatures below 1100°C has proven to be a serious obstacle to its more widespread use. Because of its high viscosity, the solution does not flow freely from the epitaxial film and the substrate holder as they are withdrawn from the melt. A film of solution nearly always clings to the wafer. If the solvent film is more than a few microns thick it can cause the epitaxial film and even the substrate to crack as it cools to room temperature.

Although garnet is congruently saturating in the BaO solvent system, the Hewlett-Packard workers[Ref. 16] obtained their best results using solutions slightly rich in rare-earth oxides; that is, toward the orthoferrite side of the stoichiometric garnet composition. (It will be recalled that the

phase relationships in the PbO solvent require that the solution contain an excess of Fe_2O_3). A solution composition similar to that used at Hewlett-Packard was used here to deposit the nominal composition $Eu_1Er_2Fe_{4.3}Ga_{0.7}O_{12}$ on (111) $Gd_3Ga_5O_{12}$ substrates. The solution composition is given in Table X. Note that BaO was weighed as $BaCO_3$. The solvent components alone were first slowly heated to about 1200°C to allow the $BaCO_3$ to decompose. The solution was then cooled and the solute components were added. The solution was maintained at about 1175°C overnight. The solution was stirred vigorously and then cooled to growth temperature.

The conditions and the results of the epitaxial film growth runs are summarized in Table XI. After each run the solution was heated to about 1075°C and stirred in preparation for the next run. The fluidity of the of solution increased with growth temperature but in no case did the solvent drain completely from the wafer. The film of solvent caused each of the wafers to crack as the wafers cooled from growth temperature to room temperature. When the solvent was removed by dissolving in warm, dilute HNO_3, the wafers usually crumbled into small pieces.

In light of these experiments and results it appeared that a considerable effort would be required to develop the techniques necessary to grow device quality films from the BaO-based flux. Furthermore, device quality films were already being grown from the $PbO-B_2O_3$ solvent. Therefore, it was decided that a continued effort with the BaO solvent would not meet the intent of the contract and work was discontinued with this solvent system.

TABLE X

Solution Composition for Growth of

$Eu_1 Er_2 Fe_{4.3} Ga_{0.7} O_{12}$ From BaO - $B2O_3$ - $Ba F_2$

Compound	Weight (gm)	Moles	Mole Percent
$BaCO_3$	24.5	0.12	32.4
B_2O_3	8.6	0.12	32.4
BaF_2	9.5	0.054	14.9
Er_2O_3	7.9	0.021	5.7
Eu_2O_3	3.9	0.011	3.0
Fe_2O_3	5.6	0.035	9.5
Ga_2O_3	1.1	0.0059	1.6

TABLE XI

Summary of Runs in BaO - B$_2$O$_3$ - BaF$_2$ Solvent

Run Number	Growth Temperature (°C)	Growth Time (min)	Remarks - Results
4435 A	959	10	Solution precipitated before run was over - solvent did not drain - wafer badly cracked
4435 B	1000	30	Solvent did not drain - wafer badly cracked - thick faceted layer
4435 C	1026	30	Solvent did not drain completely wafer badly cracked - thick faceted layer
4435 D	1054	30	Thin film of solvent on layer wafer cracked - thick faceted layer
4435 E	1054	10	Thin film of solvent on layer wafer cracked - thin layer

5. CONCLUSIONS AND RECOMMENDATIONS

Crystals of $Gd_3 Ga_5 O_{12}$ of high structural quality have been grown by the Czochralski method. Polished wafers sliced from these crystals exhibit less than 10 dislocations/cm^2. The low dislocation crystals grown to date at Monsanto have exhibited coring and growth striations. Epitaxial films grown on these substrates also exhibit striations corresponding to those in the substrate. Liquid phase epitaxial growth conditions can be adjusted to minimize the replication of the substrate striations to the extent that they have little or no effect on the propagation of magnetic domains. Nevertheless, core-free, striation-free wafers are preferred substrates. Recently, at least two commercial suppliers of $Gd_3 Ga_5 O_{12}$ (Union Carbide and Airtron) have begun to market core-free, low dislocation $Gd_3 Ga_5 O_{12}$ and it is expected that this material will soon be available generally.

A polishing procedure which produces work damage-free surfaces has been developed for (111) $Gd_3 Ga_5 O_{12}$ substrates. The final step involves removing 1 to 2 mils of the substrate on a Syton-flooded, Corfam lap. The procedure produces an excellent surface for epitaxial growth. However, the final polishing results in considerable rounding of the substrate edges. It is recommended tha polishing procedures be reevaluated frequently to insure that surface preparation contributes to and is kept abreast of advances in film growth technology. Of specific current importance is a polishing procedure which will produce a flat and damage-free surface.

Device quality, magnetic bubble films of a number of compositions have been deposited on $Gd_3 Ga_5 O_{12}$ substrates by the dipping method from a supercooled $PbO-B_2O_3$ solution. The relatively low viscosity of the $PbO-B_2O_3$ solvent compared to BaO oxide solvents at epitaxial growth temperatures below 1000°C has proven to be a telling advantage for the use of this solvent system.

Epitaxial films of six different compositions were delivered to ARPA. These include films of Super IV, Super VIII and four different compositions of the Super V family. Super IV and Super VIII garnets exhibit growth induced anisotropy while the anisotropy of the Super IV garnets is primarily stress induced. Domain wall mobility in all the Super V garnets exceeded 200 cm/Oe-sec. No clear-cut relations between film composition and mobility were found. However, mobility did tend to decrease from composition to composition with increasing anisotropy as is expected.

The investigation of the preparation of magnetic bubble films by ARC-plasma spraying and by chemical vapor deposition will be included in the next phase of this program. The preparation of films by LPE will be continued also. It is recommended that the LPE effort be devoted to studies of additional compositions of the Super V family. The Eu-Y system is of particular interest because of its reported temperature stability[Ref. 15].

6. REFERENCES

1. Monsanto Research Corp., "Magnetic Bubble Materials, Initial Characterization Report" Contract No. DAAH01-72-C-0490, (March 1972).

2. Roger W. Shaw, Robert M. Sandfort and Jerry W. Moody, "Magnetic Bubble Materials - Characterization Techniques Study Report" Contract No. DAAH01-72-C-0490, (July 1972).

3. B. Cockayne, M. Chesswass and D. B. Gasson, "The Growth of Strain Free $Y_3Al_5O_{12}$ Single Crystals", J. Mater. Sci. 3, 224, (1968).

4. C. D. Brandle and A. J. Valentino, "Czochralski Growth of Rare-Earth Gallium Garnets", J. Cryst. Growth, 12, 3, (1972).

5. D. F. O'Kane and V. Sadagopan, "Crystal Growth and Characterization of Gadolinium Gallium Garnet", Paper No. 9, Electrochemical Society Meeting, Houston, Texas 1972.

6. R. C. Linares, "Growth of Garnet Saser Crystals", Sol. State Comm. 2, 229, (1964).

7. C. D. Brandle, D. C. Miller and J. W. Nielsen, "The Elimination of Defects in Czochralski Grown Rare-Earth Gallium Garnets" J. Cryst. Growth. 12, 195 (1972).

8. P. J. Besser, J. E. Mee, P. E. Elkins and D. M. Heinz, "A Stress Model for Heteroepitaxial Magnetic Oxide Films Grown by Chemical Vapor Deposition", Mat. Res. Bull. 6, 1111, (1971).

9. L. K. Shick, J. W. Nielsen, A. H. Bobeck, A. J. Kurtzig, P. C. Michaelis and J. P. Reekstein, "Liquid Phase Epitaxial Growth of Uniaxial Garnet Films; Circuit Deposition and Bubble Propogation" App. Phys. Letters 18, 89 (1971).

10. R. Hiskes, T. L. Felmlee and R. A. Burmeister, "Growth of Rare-Earth Orthoferrites and Garnets Using BaO-Based Solvents", Paper No. 2, Technical Conference of Met. Soc. of AIME, San Francisco, Calif. (1971).

11. H. J. Levenstein and R. W. Landorf, "Rapid Technique for Hetero-epitaxial Growth of Thin Magnetic Garnet Films", Paper 10.4, Intermag Conference, Denver, Colorado (1971).

12. W. H. Grodkiewicz, E. F. Dearborn and L. G. Van Uitert, "Growth of Large Yttrium and Rare Earth Aluminum and Iron Garnets", Crystal Growth, p. 441, Pergamon Press, New York (1967).

13. J. W. Nielsen and E. F. Dearborn, "The Growth of Single Crystals of Magnetic Garnets", J. Phys. Chem. Solids 5, 202 (1958).

14. H. J. Levenstein, S. Licht, R. W. Landorf and S. L. Blank, "Growth of High Quality Garnet Thin Films from Supercooled Melts", App. Phys. Letters 19, 486 (1971).

15. F. A. Giess, B. E. Argyle, D. C. Cranemeyer, E. Klakholm, T. R. McGuire, D. F. O'Kane, T. S. Plaskett and V. Sadagopan, "Europium-Yttrium Iron-Gallium Garnet Films Grown by Liquid Phase Epitaxy on Gadolinium Gallium Garnet", Paper 2C-5, 17th Conf. Mag. and Mag. Mat. Chicago, Ill. (Nov. 1971).

16. R. A. Burmeister, T. L. Felmlee and R. Hiskes, "Magnetic Rare-Earth Compounds", Semiannual Technical Report, Contract No. DAAH01-70-C-1106 Program Code No. OD10, December 1970.

17. A. H. Bobeck, D. H. Smith, E. G. Spencer, L. G. Van Uitert and E. M. Walters, "Magnetic Properties of Flux Grown Uniaxial Garnets", IEEE Trans. Mag. , 461 (1971).

18. R. C. Linares, "Growth of Yttrium Iron Garnet from Molten Barium Borate", J. Am. Ceram. Soc. 45, 307 (1962).

19. R. A. Laudise, R. C. Linares and E. F. Dearborn, "Growth of Yttrium Iron Garnet of a Seed from a Molten Salt Solution", J. App. Phys., 33 Suppl, 1362 (1962).

APPENDIX A

Some Properties of Rare Earth Iron and Gallium Garnets

APPENDIX A-1

Properties of the Rare Earth Magnetic Garnets

Garnet	Lattice Constant (Å)	Saturation Magnetization (gauss)	Magnetostriction Coefficients		Compensation Temperature (°K)	Neel Temperature (°K)
			$\lambda(111) \times 10$	$\lambda(100) \times 10$		
$Sm_3Fe_5O_{12}$	12.530	1675	− 8.5	+21		578
$Eu_3Fe_5O_{12}$	12.498	1172	+ 1.8	+21		566
$Gd_3Fe_5O_{12}$	12.479	56	− 3.1	0	290	564
$Tb_3Fe_5O_{12}$	12.447	198	+12.0	− 3.3	246	568
$Dy_3Fe_5O_{12}$	12.408	376	− 5.9	−12.5	220	563
$Ho_3Fe_5O_{12}$	12.380	882	− 4.0	− 3.4	136	567
$Er_3Fe_5O_{12}$	12.349	1241	− 4.9	+ 2.0	84	556
$Tm_3Fe_5O_{12}$	12.325	1397	− 5.2	+ 1.4	<20	549
$Yb_3Fe_5O_{12}$	12.291	1555	− 4.5	+ 1.4	~ 0	548
$Lu_3Fe_5O_{12}$	12.277	1815	− 2.4	− 1.4		549
$Y_3Fe_5O_{12}$	12.377	1767	− 2.4	− 1.4		560

Lattice Constants of the Rare Earth Gallium Garnets

Garnet	Lattice Constant Å
$Pr_3Ga_5O_{12}$	12.570
$Nd_3Ga_5O_{12}$	12.506
$Sm_3Ga_5O_{12}$	12.432
$Eu_3Ga_5O_{12}$	12.401
$Gd_3Ga_5O_{12}$	12.383
$Tb_3Ga_5O_{12}$	12.348
$Dy_3Ga_5O_{12}$	12.307
$Ho_3Ga_5O_{12}$	12.293
$Er_3Ga_5O_{12}$	12.255
$Tm_3Ga_5O_{12}$	12.225
$Yb_3Ga_5O_{12}$	12.204
$Lu_3Ga_5O_{12}$	12.188
$Y_3Ga_5O_{12}$	12.280

APPENDIX B

LPE Growth Parameters for Rare Earth Magnetic Garnets

APPENDIX B-1

Growth Parameters for Eu-Er Garnets

Solution Composition:

Compound	Weight (gm)	Mole	Mole Percent
Eu_2O_3	0.20	0.00057	0.12
Er_2O_3	0.83	0.0022	0.48
Fe_2O_3	5.00	0.031	6.7
Ga_2O_3	0.45	0.0024	0.52
PbO	90.0	0.40	86.5
B_2O_3	1.8	0.026	5.7

Saturation Temperature : $\approx 930°C$

Growth Temperature : $890°C*$

Growth Rate : $\approx 0.38 \,\mu m/min$

Film Composition : $Eu_{0.63} Er_{2.27} Fe_{4.36} Ga_{0.64} O_{12}$

* Note: Films may contain some Pb when grown at this temperature.

Growth Parameters for Gd-Er Garnets

Solution Composition:

Compound	Weight (gm)	Mole	Mole Percent
Gd_2O_3	0.4519	0.001249	0.18
Er_2O_3	1.3135	0.003435	0.49
Fe_2O_3	7.6755	0.04807	6.88
Ga_2O_3	0.4744	0.002531	0.36
PbO	135.0	0.6048	86.54
B_2O_3	2.700	0.03877	5.55

Saturation Temperature : $\approx 940°C$

Growth Temperature : $900°C$

Growth Rate : $\approx 0.22 \ \mu m/min$

Film Composition : $Gd_{0.9} Er_{2.1} Fe_{4.55} Ga_{0.45} O_{12}$

Growth Parameters for G-Y Garnets

Solution Composition:

Compound	Weight (gm)	Mole	Mole Percent
Gd_2O_3	0.3119	0.0008621	0.13
Y_2O_3	1.1035	0.004886	0.70
Fe_2O_3	8.2666	0.05177	7.47
Ga_2O_3	1.2092	0.006451	0.93
PbO	132.0	0.5919	85.39
B_2O_3	2.600	0.03733	5.38

Saturation Temperature : $\approx 110°C$

Growth Temperature : $976°C$

Growth Rate : $\approx 0.36 \ \mu m/min$

Film Composition : $Gd_{0.46} Y_{2.54} Fe_{3.95} Ga_{1.05} O_{12}$

APPENDIX B-4

Growth Parameters for Gd-Yb-Y Garnets

Solution Composition:

Compound	Weight (gm)	Mole	Mole Percent
Gd_2O_3	0.3839	0.001061	0.22
Yb_2O_3	0.4575	0.001160	0.25
Y_2O_3	0.3726	0.001650	0.35
Fe_2O_3	5.6527	0.03540	7.51
Ga_2O_3	0.6164	0.003289	0.70
PbO	90.00	0.4032	85.50
B_2O_3	1.800	0.02585	5.48

Saturation Temperature : $\approx 1000°C$

Growth Temperature : $946°C$

Growth Rate : $\approx 0.47 \; \mu m/min$

Film Composition : $Gd_{0.99} \; Y_{1.15} \; Yb_{0.86} \; Fe_{4.16} \; Ga_{0.84} \; O_{12}$

75

APPENDIX B-5

Growth Parameters for Gd-Tm-Y Garnets

Solution Composition:

Compound	Weight (gm)	Mole	Mole Percent
Gd_2O_3	0.3622	0.001001	0.21
Tm_2O_3	0.5926	0.001532	0.32
Y_2O_3	0.2261	0.001001	0.21
Fe_2O_3	5.7740	0.03616	7.64
Ga_2O_3	0.5102	0.002722	.94
PbO	90.00	0.4032	85.21
B_2O_3	1.800	0.02585	5.46

Saturation Temperature : $\approx 980°C$

Growth Temperature : $950°C$

Growth Rate : $\approx 0.24\ \mu m/min$

Film Composition : $Gd_{1.09}\ Tm_{0.93}\ Y_{0.98}\ Fe_{4.32}\ Ga_{0.68}\ O_{12}$

APPENDIX B-6

Growth Parameters for Gd-La-Y Garnets

Solution Composition:

Compound	Weight (gm)	Mole	Mole Percent
Gd_2O_3	0.1279	0.0003535	.068
La_2O_3	0.0653	0.0002004	.039
Y_2O_3	0.6732	0.002901	0.57
Fe_2O_3	5.5249	0.03460	6.67
Ga_2O_3	0.8017	0.004277	0.82
PbO	100.0	0.4480	86.30
B_2O_3	2.000	0.02872	5.53

Saturation Temperature : $\approx 985°C$

Growth Temperature : $944°C$

Growth Rate : $\approx 0.26 \ \mu m/min$

Film Composition : $Gd_{0.44} \ La_{0.04} \ Y_{2.52} \ Fe_{4.01} \ Ga_{0.99} \ O_{12}$

APPENDIX C

Characterization Data of Bubble Films

APPENDIX C

Characterization Data of Bubble Films

Composition	Sample Number	h	ℓ	$4\pi M_s$	H_C	H_A	μ	T_N	H_{S-B}	d_{S-B}	H_0	d_0	σ_w
$Eu_{0.62}Er_{2.38}Fe_{4.42}Ga_{0.58}O_{12}$	EuEr-1	3.34	0.51	308	0.44	5500	15	461	64	7	142	3	0.38
	EuEr-2	7.94	0.50	344	0.20	5500	22	460	179	7	210	2	0.47
$Eu_{0.62}Er_{2.38}Fe_{4.36}Ga_{0.64}O_{12}$	EuEr-3	5.79	0.68	278	0.68	5500	13	459	95	7	136	3	0.42
	EuEr-4	5.88	0.68	278	0.68	5500	18	459	95	7	136	3	0.42
$Eu_{0.7}Er_{2.3}Fe_{4.35}Ga_{0.65}O_{12}$	EuEr-5	9.98	0.50	304	0	5500	22	460	170	9	203	3	0.37
	EuEr-6	5.61	1.16	196	0.61	5400	17	454	58	9	75	3	0.35
$Gd_{0.8}Er_{2.2}Fe_{4.56}Ga_{0.44}O_{12}$	GdEr-1	3.76	0.81	171	0.05	1310	60	479	46	9	65	3	0.19
	GdEr-2	10.4	0.69	177	0.09	1540	90	481	96	11	110	4	0.17
	GdEr-3	2.96	0.88	151	0.07	1470	120	480	36	11	43	4	0.16
	GdEr-4	5.27	3.57	213	0.05	1390	95	482	97	9	117	3	0.21
	GdEr-5	4.60	0.63	198	0.11	1400	79	481	79	8	98	3	0.20
$Gd_{0.46}Y_{2.54}Fe_{3.95}Ga_{1.05}O_{12}$	GdY-1	5.14	0.49	148	0.15	370	540	418	59	6	82	2	0.85
	GdY-2	5.00	0.45	142	0.07	350	400	417	66	6	80	2	0.72
	GdY-3	4.04	0.52	142	0.20	370	500	417	55	6	69	2	0.83
	GdY-4	4.64	0.42	140	0.16	340	460	419	62	6	73	2	0.66
	GdY-5	4.60	0.49	131	0.06	350	400	418	58	6	70	2	0.67
$Gd_{0.99}Yb_{0.86}Y_{1.15}Fe_{4.16}Ga_{0.84}O_{12}$	GdYYb-1	5.47	0.52	158	0.05	560	260	459	70	7	87	2	0.10
	GdYYb-2	5.74	0.48	170	0.05	600	540	459	79	7	98	2	0.11
	GdYYb-3	5.25	0.55	148	0.05	600	380	458	66	8	81	2	0.10
	GdYYb-4	5.71	0.53	161	0.05	640	640	458	75	8	90	3	0.11
	GdYYb-5	5.10	0.57	168	0.13	660	800	459	63	8	79	2	0.13
$Gd_{0.44}La_{0.04}Y_{2.52}Fe_{4.01}Ga_{0.99}O_{12}$	GdYLa-1	3.91	0.69	118	0.11	570	330	410	37	9	49	2	0.076
	GdYLa-2	3.77	0.70	117	0.09	570	360	410	36	8	47	3	0.076
	GdYLa-3	4.16	0.70	114	0.13	560	390	410	35	8	49	2	0.072
	GdYLa-4	4.20	0.70	110	0.17	560	410	410	35	8	47	2	0.068
	GdYLa-5	4.05	0.72	113	0.13	560	540	410	35	9	47	2	0.073
$Gd_{1.09}Tm_{0.93}Y_{0.98}Fe_{4.32}Ga_{0.68}O_{12}$	GdYTm-1	5.23	0.72	158	0.07	1160	390	475	56	10	74	3	0.14
	GdYTm-2	5.31	0.69	157	0.13	1160	440	474	58	9	77	2	0.14
	GdYTm-3	4.57	0.72	163	0.20	1160	220	474	54	10	73	2	0.15
	GdYTm-4	4.41	0.74	163	0.15	1160	240	474	49	9	69	2	0.16
	GdYTm-5	6.03	0.71	162	0.15	1160	210	474	64	10	82	3	0.15

Legend

h	Thickness, μm
ℓ	Characteristic Length, μm
$4\pi M_s$	Saturation Magnetization, gauss
H_C	Coercivity, Oe
H_A	Anisotropy, Oe
μ	Mobility, cm/sec/Oe
T_N	Neel Temperature, °K
H_{S-B}	Strip to Bubble Transition filed, Oe
d_{S-B}	Bubble diameter at H_{S-B}, μm
H_0	Bubble collapse field, Oe
d_0	Bubble diameter at H_0, μm
σ_w	Domain wall energy/unit area, ergs/cm^2